



MINISTÉRIO DA EDUCAÇÃO  
UNIVERSIDADE FEDERAL RURAL DA AMAZÔNIA  
PROGRAMA DE PÓS-GRADUAÇÃO EM AGRONOMIA

**PEDRO PAULO DA COSTA ALVES FILHO**

**Risco ambiental e à saúde humana de elementos potencialmente tóxicos em resíduos de áreas de mineração artesanal de cassiterita e monazita na Amazônia**

**Belém**  
**2024**



MINISTÉRIO DA EDUCAÇÃO  
UNIVERSIDADE FEDERAL RURAL DA AMAZÔNIA- UFRA  
PROGRAMA DE PÓS-GRADUAÇÃO EM AGRONOMIA

**PEDRO PAULO DA COSTA ALVES FILHO**

**Risco ambiental e à saúde humana de elementos potencialmente tóxicos em resíduos de áreas de mineração artesanal de cassiterita e monazita na Amazônia**

**Tese apresentada à Universidade Federal Rural da Amazônia, Programa de Pós-Graduação em Agronomia, como parte das exigências para obtenção do título de Doutor em Agronomia.**

**Orientador: Antonio Rodrigues Fernandes, Dr.**

**Coorientadores: Silvio Junio Ramos, Dr.**

**Edna Santos de Souza, Dra.**

**Belém  
2024**

**PEDRO PAULO DA COSTA ALVES FILHO**

**Risco ambiental e à saúde humana de elementos potencialmente tóxicos em resíduos de áreas de mineração artesanal de cassiterita e monazita na Amazônia**

Tese apresentada à Universidade Federal Rural da Amazônia, Programa de Pós-Graduação em Agronomia, como parte das exigências para obtenção do título de Doutor em Agronomia.

Orientador: Antonio Rodrigues Fernandes, Dr.

Coorientadores: Silvio Junio Ramos, Dr.

Edna Santos de Souza, Dra.

**29 de novembro de 2024.**

**Data da aprovação**

**BANCA EXAMINADORA**

---

**Dr. Antonio Rodrigues Fernandes - Orientador**

**UNIVERSIDADE FEDERAL RURAL DA AMAZÔNIA – UFRA**

---

**Ana Regina da Rocha Araújo, Dr<sup>a</sup>. 1<sup>a</sup> Examinadora.**

**UNIVERSIDADE FEDERAL RURAL DA AMAZÔNIA**

---

**Jessivaldo Rodrigues Galvão, Dr. ° Examinador.**

**UNIVERSIDADE FEDERAL RURAL DA AMAZÔNIA**

---

**Matheus Bortolanza Soares, Dr 3º Examinador.**

**UNIVERSIDADE DE SÃO PAULO**

---

**Cristine Bastos do Amarante, Dr<sup>a</sup>. 4<sup>a</sup> Examinadora.**

**MUSEU EMILIO GOELDI**

## **AGRADECIMENTOS**

Agradeço a Deus;

À Universidade Federal Rural da Amazônia (UFRA) pela formação e suporte proporcionados em 11 anos de ensino;

Ao Programa de Pós-graduação em Agronomia (PGAGRO), pela oportunidade;

À CAPES pela concessão da minha bolsa de estudos e ao CNPq pelo financiamento desta pesquisa;

Ao meu orientador, professor Dr. Antonio Rodrigues Fernandes, por todo o aprendizado acadêmico e de vida, as ideias e sugestões compartilhadas, aos puxões de orelha e paciência nesses 4 anos de orientação;

Ao Dr. Sílvio Júnio Ramos do Instituto Tecnológico Vale (ITV) e a doutora Edna Santos de Souza, meus coorientadores por contribuir de maneira significativa com o desenvolvimento desta pesquisa;

A minha companheira Lorryne Moraes, por todo companheirismo no decorrer de minha vida acadêmica e pessoal;

A minha filha, Lara Alves, por ter se tornado o maior motivo para seguir em frente;

Aos meus pais, Pedro Alves e Círia Alves, meu eterno agradecimento por todo esforço em me proporcionar os ensinamentos necessários ao longo da vida;

Aos eternos amigos de Graduação e Engenheiros agrônomos, Leonardo Neves e Igor Costa;

Ao Dr. Yan Nunes pela amizade e tão importante parceria para a conclusão dos nossos trabalhos;

Ao Dr. Wendell Pereira, pelo apoio e contribuições técnicas;

Aos sempre prestativos colegas de LETAM, Adrielle Laena, Gabriela Almeida e Flávio Rodrigues pelo apoio e amizade.

As estagiárias do LETAM, Anna Amaral, Luana Ferreira.

## **RESUMO**

A exploração mineral é essencial para o desenvolvimento econômico mundial. Na região amazônica, a exploração artesanal é predominante e realizada em grande escala, sem preocupação com os impactos ambientais e a saúde humana, principalmente devido a liberação de grandes quantidades de elementos potencialmente tóxicos (EPTs) (neste trabalho representado pelos metais e metaloides) e elementos terras raras (ETRs). No capítulo 1 os objetivos foram quantificar as concentrações de Elementos de Terras Raras (ETRs) e estimar os riscos ambientais e à saúde humana em áreas de mineração artesanal de cassiterita e monazita na região amazônica, bem como compreender a dinâmica desse risco ao longo do tempo após a exploração. Foram avaliados o risco ao ambiente e a saúde humana em resíduos (estéril e rejeito) de três áreas de mineração artesanal de cassiterita e monazita, em função do tempo de exploração. No capítulo 2 o objetivo foi quantificar as concentrações de EPTs e estimar a contaminação e poluição ambiental em áreas de mineração artesanal de cassiterita na região amazônica. Assim, foram estimados índices de risco ambiental e a saúde humana de EPTs que apresentaram concentração acima do valor de referência de qualidade para o estado do Pará. As concentrações de ETRs e EPTs foram quantificadas por fusão alcalina e ICP-MS. Os resultados foram utilizados para calcular índices de poluição, risco ambiental e a saúde humana. Os resíduos da exploração de monazita e cassiterita provocaram o aumento das concentrações ETRs e EPTs, elevado enriquecimento e alto fator de contaminação por EPTs e ETRs. Os resíduos das minas ativas e recentemente desativadas apresentaram elevado risco ecológico. Os resultados indicam que a mineração artesanal de cassiterita e monazita tem potencial de contaminação e enriquecimento por EPTs e ETRs. A considerável bioacumulação em plantas forrageiras, indica alto risco potencial em um município que é o maior produtor de rebanho bovino do país. A partir destes resultados podemos concluir que medidas de monitoramento e remediação devem ser tomadas pelas autoridades estaduais que cuidam do meio ambiente.

### **Palavras-chave:**

Elementos de terras raras, propriedades químicas, biodisponibilidade, metais e metaloides, índices de poluição.

## **ABSTRACT**

Mineral exploration is essential for global economic development. In the Amazon region, artisanal mining is predominant and conducted on a large scale, with little regard for environmental impacts and human health, primarily due to the release of large amounts of potentially toxic elements (PTEs), including rare earth elements (REEs). Rare earth elements (REEs) include the lanthanide family, scandium, and yttrium, and are essential for sustaining modern technologies. In the region of São Felix do Xingu, located in the Amazonian craton, there are minerals containing rare earth elements, including monazite and cassiterite. In Chapter 1, the risk to the environment and human health was assessed in waste (overburden and tailings) from three artisanal mining areas of cassiterite and monazite, based on the length of exploitation. In Chapter 2, environmental and human health risk indices were estimated for PTEs (metals and metalloids) that showed concentrations above the quality reference values for the state of Pará. REE and PTE concentrations were quantified by alkaline fusion and ICP-MS. The results were used to calculate pollution, environmental risk, and human health indices. Waste from monazite and cassiterite mining led to increased concentrations of REEs and PTEs, with high enrichment and a high contamination factor for REEs and PTEs. Waste from active and recently deactivated mines showed high ecological risk. The results indicate that artisanal cassiterite and monazite mining has potential for PTE and REE contamination and enrichment. The significant bioaccumulation in forage plants indicates a high potential risk in a municipality that is the largest producer of cattle in the country. Therefore, regulatory and damage mitigation measures need to be considered.

### **Key words:**

**Rare earth elements, chemical properties, bioavailability, metals and metalloids, pollution indices.**

<b>Sumário</b>	
RESUMO	5
ABSTRACT	6
Rare earth elements, chemical properties, bioavailability, metals and metalloids, pollution indices.	6
Sumário	9
CONTEXTUALIZAÇÃO	10
REFERÊNCIAS	12
<b>CAPÍTULO 1</b>	16
Artisanal mining of monazite and cassiterite in the Amazon: Potential risks of rare earth elements for the environment and human health	16
ABSTRACT	16
1. INTRODUCTION	17
2. MATERIAL AND METHODS	19
2.2. Chemical Characterization of samples	21
2.4 Pollution assessment	22
2.5 Environmental risk assessment	24
2.6 Human health risk assessment	25
2.7 Statistical analyzes	26
3.2. Concentrations, fractionation and geochemical signatures of REEs	29
3.3. Relationship between variables	34
3.4. Pollution índices	35
3.5. Environmental risks	40
3.6. Human health risks	42
4. CONCLUSIONS	43
REFERENCES	45
SUPPLEMENTARY MATERIAL	60
<b>CAPÍTULO 2</b>	68
Resíduos da mineração artesanal de cassiterita na Amazônia: riscos ambientais e a saúde humana	68
1. INTRODUÇÃO	70
2. MATERIAL E MÉTODOS	71
2.1. Área de estudo e amostragem	71
2.2. Caracterização de amostras de solo, planta e fator de bioacumulação	72
2.3. Avaliação da poluição	74

2.4. Avaliação de risco ambiental	75
2.5. Risco a saúde humana	76
2.6. Análises estatísticas	77
3. RESULTADOS E DISCUSSÕES	78
3.1. Caracterização dos resíduos de mineração e concentração de EPTs	78
CONCLUSÃO	86
REFERENCES	87

## **CONTEXTUALIZAÇÃO**

A produção mineral tem grande relevância na economia mundial, no Brasil, contribui de forma significativa para a balança comercial. Por outro lado, a exploração mineral causa mudanças significativas no ambiente, alterando de forma negativa a fauna e a flora. De forma sustentável se constitui em grande desafio. A mineração tem como principal característica a retirada e escavação de solos em áreas que apresentem elevada concentração de determinado elemento mineral e concentrações variadas de outros. Esses elementos minerais se constituem em elementos potencialmente tóxicos (EPTs), mesmo em baixas concentrações, consequentemente estarão presentes nos resíduos gerados. Em função disso, a exploração mineral tem contribuído para a contaminação do solo, das águas e das plantas, e por conseguinte causando riscos à saúde humana, comprometendo os ecossistemas e a segurança alimentar (Chai *et al.*, 2015; Souza Neto *et al.*, 2020; Souza *et al.*, 2017; Xiao *et al.*, 2017).

As empresas de mineração são submetidas a legislação reguladora, cujo funcionamento é mediante medidas mitigadoras e compensatórias, que garantam um mínimo de impacto das condições ambientais. Em contrapartida a mineração artesanal, representa riscos a saúde humana e ao meio ambiente, pois, é uma atividade comumente ilegal, a exemplo a extração artesanal de ouro, que faz uso de Hg e cianeto, que são lançados no ambiente (Souza Neto et al., 2020).

Essa forma de exploração mineral faz uso de tecnologia rudimentar por indivíduos, grupos ou comunidades, predominante em países em desenvolvimento, ocorrendo em grande parte de forma ilegal, expondo a população a riscos potenciais (Pereira et al., 2020; Souza Neto et al., 2020; Teixeira et al., 2019). As práticas e efeitos da mineração artesanal de cassiterita e monazita realizada no distrito do Taboca, em São Félix do Xingu ainda não são conhecidas.

A cassiterita é um dióxido natural e principal minério de estanho ( $\text{SnO}_2$ ) de coloração variada com ocorrência na forma de cristais tetragonais. É utilizado em função da extração de Sn, que é utilizado para produção de ligas metálicas para impedir a corrosão de outros metais (Barbosa et al. 2019) A monazita é um fosfato que contém elementos de terras raras (ETRs), como, tório (potencial para revolução energética, equipamentos de laboratório, componente de ligas), lantâno (eletrodos de carbono para projeção de luz, lentes óticas e vidros absorventes de radiação) e cério (metalurgia) (Liu et al., 2013; Zhang et al., 2014).

Os ETRs são 17 elementos químicos pertencentes ao grupo dos lantanídeos adicionados o escândio (Sc) e o ítrio (Y). As principais fontes econômicas proveniente de minerais de terras raras são monazita, bastnasite, xenótimo e loparite e as argilas lateríticas (Gwenzi et al., 2018; Yuan et al., 2018). Os óxidos e minerais de terras raras estão aumentando sua procura devido ao surgimento de novas tecnologias para produção de energia limpa (United States Geological Survey 2016; Gwenzi, et al. 2018).

Atualmente as estratégias para aumentar essa oferta de ETR's baseiam se em descobrir novos depósitos, reabrir minas antigas e aumentar a produção de minas já existentes, assim se tornando um recurso estratégico. O Brasil possui as maiores reservas de ETRs do mundo. Atualmente existem três projetos de mineração de ETRs em execução e implantação no Brasil, carbonatito alcalino de Araxá (Minas Gerais), Projeto Pitinga (Amazonas) e Projeto Serra Dourada na província de estanho de Goiás (Takehara et al., 2015).

Os rejeitos normalmente contêm altas concentrações de elementos potencialmente tóxicos (EPTs) residuais, os quais são poluentes persistentes nos solos, sedimentos e águas, e que podem ser absorvidos e acumulados em organismos e representar toxicidade significativa para os consumidores no topo das cadeias alimentares (Looi et al., 2018).

Os EPT's se originam de fontes litogênicas via pedogênese, e de fontes antropogênicas, como a mineração, uso de pesticidas, bioassólidos fosseis, combustão de combustíveis e atividades industriais. Quando presentes por via litogênica, apresenta baixa concentração dos elementos e baixo risco a saúde humana, quando por via antropogênica apresentam altas concentrações (Fernandes et al, 2018).

O conhecimento sobre contaminação por substâncias tóxicas inorgânicas na Amazônia é essencial para os órgãos de supervisão ambiental e de saúde pública, pois esta região possui a maior concentração de biodiversidade do mundo e o maior potencial de mineração do Brasil (entre as de maior expressão mundial) (Souza et al, 2017). O acúmulo de EPT's em organismos vivos através da cadeia alimentar e ingestão de água representa ameaça a vida humana e equilíbrio dos ecossistemas (Tóth et al, 2016, Souza Neto et al, 2020).

Logo, a determinação da concentração de elementos com potencial de toxidez e poluentes emergentes, além da estimativa de riscos ambientais e a saúde humana se tornam métricas imprescindíveis para um planejamento de medidas mitigatórias no processo de exploração desses minerais, devido a exposição aos possíveis contaminantes.

## **Hipóteses**

Capítulo 1: Os resíduos de mineração artesanal de monazita e cassiterita apresentam concentrações de elementos terras raras que representem riscos a saúde humana e ao ambiente.

Capítulo 2: O resíduo da exploração realizada em São Félix do Xingú para obtenção de ETRs, gera a concentração de outros elementos potencialmente tóxicos, como metais pesados, representando risco ao meio ambiente.

## **Objetivos**

Capítulo 1: Os objetivos foram quantificar as concentrações de Elementos de Terras Raras (ETRs) e estimar os riscos ambientais e à saúde humana em áreas de mineração artesanal de cassiterita e monazita na região amazônica, bem como compreender a dinâmica desse risco ao longo do tempo após a exploração.

Capítulo 2: o objetivo foi quantificar as concentrações de EPTs e estimar a contaminação e poluição ambiental em áreas de mineração artesanal de cassiterita na região amazônica, além de determinar a bioacumulação desses elementos em plantas de *B. brizantha*.

## Referencial Bibliográfico

BARBOSA, N; TEIXEIRA, W; ÁVILA, C. A.; MONTECINOS, P. M.; BONGIOLO, E. M; VASCONCELOS, F.F. U-Pb geochronology and coupled Hf-Nd-Sr isotopic-chemical constraints of the Cassiterita Orthogneiss (2.47–2.41-Ga) in the Mineiro belt, São Francisco craton: Geodynamic fingerprints beyond the Archean-Paleoproterozoic Transition, Precambrian Research, Volume 326, 2019, Pages 399-416. <https://doi.org/10.1016/j.precamres.2018.01.017>.

BONANNO, G., LO GIUDICE, R., 2010. Heavy metal bioaccumulation by the organs of Phragmites australis (common reed) and their potential use as contamination indicators. Ecol. Indic. 10:639–645.  
<http://dx.doi.org/10.1016/j.ecolind.2009.11.002>

CHAI, Y., GUO, J., CHAI, SH., CAI, J., XUE, L., ZHANG, Q. 2015. Source identification of eight heavy metals in grassland soils by multivariate analysis from the Baicheng–Songyuan area, Jilin Province, Northeast China. Chemosphere 134, 67–75. <http://dx.doi.org/10.1016/j.chemosphere.2015.04.008>.

COVRE, W. P.; PEREIRA, W. V. da S.; GONÇALVES, D. A. M.; TEIXEIRA, O. M. M.; AMARANTE, C. B. do; FERNANDES, A. R. Phytoremediation potential of *Khaya ivorensis* and *Cedrela fissilis* in copper contaminated soil. *Journal of environmental management*, v. 268, p. 110733, 2020.

CHU, S., JACOBS, D.F., LIAO, D. LIANG, L. L.; WU, D.; CHEN, LAI, C.; ZHONG, F.; ZENG, S. Effects of landscape plant species and concentration of sewage sludge compost on plant growth, nutrient uptake, and heavy metal removal. *Environ Sci Pollut Res* 25, 35184–35199 (2018). <https://doi.org/10.1007/s11356-018-3416-x>

DE SOUZA, E. S.; TEIXEIRA, R. A.; COSTA, H. S. C.; OLIVEIRA, F. J.; MELO, L. C. A.; FAIAL, K. C. F.; FERNANDES, A. R. Assessment of risk to human health from simultaneous exposure to multiple contaminants in an artisanal gold mine in Serra Pelada, Pará, Brazil. *Science of the total environment*, v. 576, p. 683-695, 2017.

DE SOUZA, E. S.; DIAS, Y. N.; DA COSTA, H. S. C.; PINTO, D. A.; DE OLIVEIRA, D.; de S. F., N.; TEIXEIRA, R. A.; FERNANDES, A. R. Organic residues and biochar to immobilize potentially toxic elements in soil from a gold mine in the Amazon. *Ecotoxicology and environmental safety*, v. 169, p. 425-434, 2019.

FERNANDES, A. R.; SANTOS, E. S.; DE SOUZA BRAZ, A. M.; BIRANI, S. M. ; ALLEONI, L. R. F. Quality reference values and background concentrations of potentially toxic elements in soils from the Eastern Amazon, Brazil. *JOURNAL OF GEOCHEMICAL EXPLORATION*, v. 190, p. 453-463, 2018.

FERNANDES, C. M. D.; GALARZA, M. A.; DE GOUVÉA, R. C. T.; DE SOUZA, H. P. T. Geochemical, geochronological, and isotopic constraints for the Archean metamorphic rocks of the westernmost part of the Carajás Mineral Province,

Amazonian Craton, Brazil. JOURNAL OF SOUTH AMERICAN EARTH SCIENCES, v. 110, p. 103340, 2021.

- GWENZI, W., MANGORI, L., DANHA, C., CHAUKURA, N., DUNJANA, N., SANGANYADO, E., 2018. Sources, behaviour, and environmental and human health risks of high-technology rare earth elements as emerging contaminants. *Sci. Total Environ.* 636, 299–313. <https://doi.org/10.1016/j.scitotenv.2018.04.235>.
- HILSON, G., 2000. Barriers to implementing cleaner technologies and cleaner production (CP) practices in the mining industry: a case study of the Americas. *Miner. Eng.* 13, 699–717
- LIU, Y.X., WANG, D.S., SHI, J.X. 2013. Magnetic tuning of upconversion luminescence in lanthanide-doped bifunctional nanocrystals[J]. *Angew. Chem. Int. Ed.* 52 (16), 4366–4369. <https://doi.org/10.1002/anie.201209884>.
- NETO, H. F. S.; PEREIRA, W. V. S.; DIAS, Y. N.; SOUZA, E. S.; TEIXEIRA, R. A. ; LIMA, M. W.; RAMOS, S. J.; AMARANTE, C. B.; FERNANDES, A. R. Environmental and human health risks of arsenic in gold mining areas in the eastern Amazon. *Environmental pollution*, v. 266, p. 114969, 2020.
- TAKEHARA, L.; Silveira, F. V.; SANTOS, R. V. Potentiality of Rare Earth Elements in Brazil. In: Borges De Lima & Leal Filho. (Org.). *Rare Earths Industry: Technological, Economic, and Environmental Implications.* 1ed. Amsterdã: Elsevier, 2015, v. 1, p. 57-68.
- TEIXEIRA, R. A.; PEREIRA, W. V. da S.; DE SOUZA, E. S.; RAMOS, S. J.; DIAS, Y. N.; DE LIMA, M. W.; DE SOUZA NETO, H. F.; DE OLIVEIRA, E. S.; Fernandes, A. R. Artisanal gold mining in the eastern Amazon: Environmental and human health risks of mercury from different mining methods. *Chemosphere*, v. 282, p. 131220, 2021.

TÓTH, G., HERMANN, T., SZATMÁRI, G., PÁSZTOR, L., 2016. Maps of heavy metals in the soils of the European Union and proposed priority areas for detailed assessment. *Sci. Total Environ.* 565, 1054–1062.

UNITED STATES GEOLOGICAL SURVEY. (2016) Mineral commodity summaries (rare earth).

YUAN, Y., CAVE, M., ZHANG, C., 2018. Using Local Moran's I to identify contamination hotspots of rare earth elements in urban soils of London. *Appl. Geochem.* 88, 167–178. <https://doi.org/10.1016/j.apgeochem.2017.07.011>.

ZHANG, X.B., WANG, L.H., ZHOU, Q., 2014. Roles of horseradish peroxidase in response to terbium stress[J]. *Biol. Trace Elem. Res.* 161 (1), 130–135. <https://doi.org/10.1007/s12011-014-0079-4>.

## CAPÍTULO 1

### Artisanal mining of monazite and cassiterite in the Amazon: Potential risks of rare earth elements for the environment and human health

Publicado no periódico Environmental management JCR: 2.7

DOI: [10.1007/s00267-024-01964-8](https://doi.org/10.1007/s00267-024-01964-8)

#### ABSTRACT

A artisanal mining is intensely applied in developing countries, and in the Amazon region, the scenario is no different. This method of mineral exploration generally does not employ mitigation techniques for potential damages and can lead to various environmental problems and risks to human health. The objectives of this study were to quantify the concentrations of Rare Earth Elements (REEs) and estimate the environmental and human health risks in artisanal mining areas for cassiterite and monazite in the Amazon region, as well as to understand the dynamics of this risk over time after exploitation. A total of 35 samples of waste classified as sterile and mining reject in active areas, as well as in areas deactivated for one and ten years, were collected. Soil samples were also collected in a forest area considered as a reference site. The concentrations of REEs were quantified using alkaline fusion and ICP-MS. The results were used to calculate pollution indices and environmental and human health risks. REEs showed higher concentrations in anthropized areas. Pollution and environmental risk levels were higher in areas deactivated for one year, with considerable contamination factors for Gd and Sm and significant to extreme enrichment factors for Sc. Human health risks were low ( $HI \leq 1$ ) in all studied areas. The results indicate that artisanal mining of cassiterite and monazite has the potential for contamination and enrichment by REEs.

**Keywords:** Environmental risk; Human health risk Contamination; Lantanídeos; Mining exploration.

## **1. INTRODUCTION**

The Amazon has the largest and most diverse reserves of minerals of commercial interest in the world, including monazite and cassiterite, which constitute important sources of rare earth elements (REEs) and tin, respectively (Neto et al., 2020). The exploration of these various minerals has significantly contributed to the region and Brazil's development. However, there have been a lot of environmental impacts associated with mineral exploration, especially in artisanal mining areas, which is normally carried out illegally, using methods with low mineral utilization, generating waste with a high potential for environmental contamination (Araújo et al., 2021; Covre et al., 2022; Lima et al., 2022; Pereira et al., 2020; Teixeira et al., 2021).

In relation to REEs, are represent a group of 17 elements (lanthanide family, plus yttrium and scandium) that have similar chemical characteristics. Despite the “rare earth” nomenclature, these elements can easily be found in abundance in the lithosphere, although the occurrence of rocks with high abundance concentrations is uncommon (Pereira et al., 2022). Concentrations of these elements in soils are regulated by the composition of the parent material, weathering processes, and soil characteristics, including texture, organic matter, and mineralogy (Mihajlovic et al., 2019). The enrichment of REEs by anthropogenic activities occurs mainly due to mineral exploration, excessive use of fertilizers and discharge of industrial and urban effluents (Atibu et al., 2018; Silva et al., 2019; Wu et al., 2019a).

The REEs are strategic and fundamental resources for the production of technological equipment, including electronic and petrochemical products, components for the renewable energy industry and national defense (Hossan et al., 2022; Zerizghi et al., 2023). Recent technological development has promoted an increase in demand for these REEs and, consequently, the growth of rocky materials mining containing these

elements. The increase in mining activity favors the accumulation of REEs in the environment, and special attention must be paid to the impacts of this activity, including contamination, ecological risks, non-carcinogenic and carcinogenic risks to human health (Cánovas et al., 2018; Liu et al., 2023; Pereira et al., 2023; Chen et al., 2022).

The city of São Félix do Xingu, located in the state of Pará (Brazilian Amazon), contains mineral reserves that are rich in REEs. In this city, several areas of artisanal monazite and cassiterite mining have produced waste (sterile waste and tailings) that can cause ecological and public health risks, especially due to the lack of measures to mitigate contamination and environmental rehabilitation. The risks caused by contamination by REEs are little known, there are reports of risk problems to the environment, and to human and animal health. La and Ce can, at high concentrations, negatively affect root growth and the mitotic index of onion bulbs (Kotelnikova et al., 2019), in addition to these effects, doses of La promoted structural modifications in cell walls and chloroplasts in soybean plants (Oliveira et al., 2015). Deleterious effects on invertebrate animals include mortality, reproductive changes and reduced locomotion (Egler et al., 2022). The presence of REEs in the blood of patients with brain tumors may be related to the brain metastasis phase (Gaman et al., 2019).

To date, these impacts have not been evaluated and studies that define environmental risks and human health are essential to support measures to protect the ecosystem and the health of the population. Therefore, the objectives were to determine the concentrations of REEs and assess the risks to the environment and human health in artisanal mining areas of cassiterite and monazite, in the southeast of the Brazilian Amazon.

## **2. MATERIAL AND METHODS**

### **2.1. Study area and sampling**

The city of São Félix do Xingu (06°37'48" S and 51°57'36" W) is located in the southeast area of the state of Pará, in the Brazilian Amazon, northern Brazil. It is the second largest municipality in Brazil in terms of territorial extension, with 84,213 km<sup>2</sup> and an estimated population of 135.732 inhabitants (IBGE, 2022). The predominant climate in the region is humid tropical, classified as Am according to the Koppen classification, with an average annual temperature of 26 °C (Alvares et al., 2013). Total annual precipitation is 1.734 mm, with rainfall concentrated in the period from November to April.

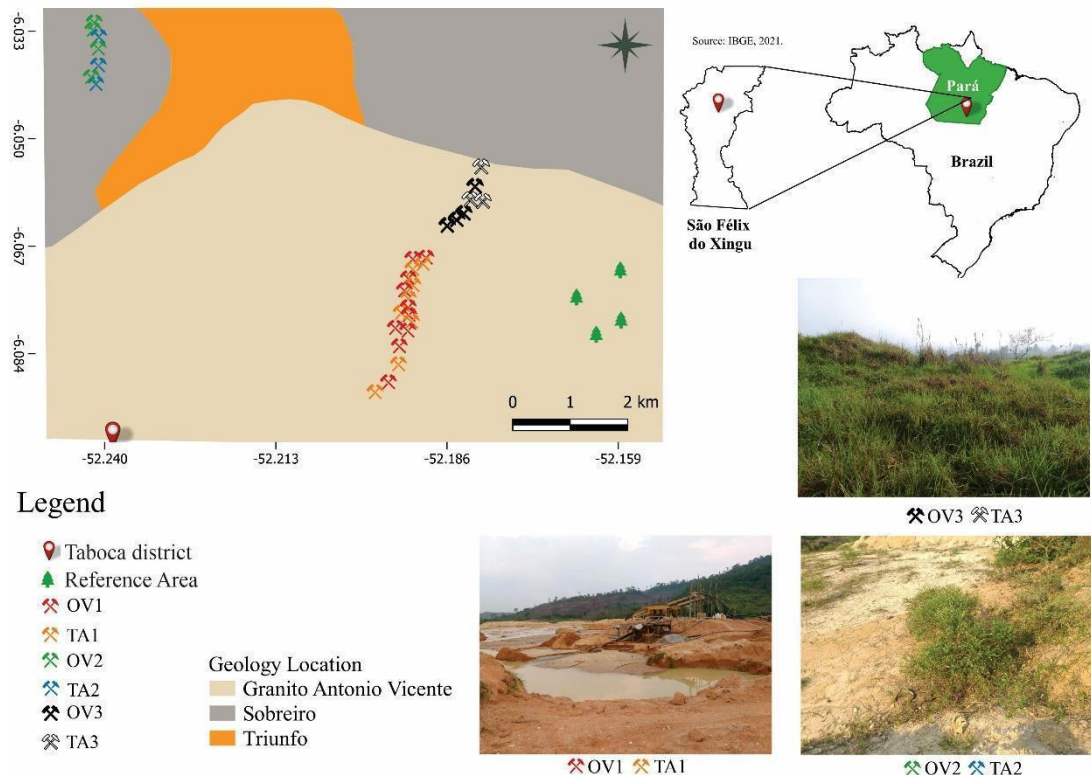
Well-preserved Paleoproterozoic volcanic-plutonic centers occur in São Félix do Xingu's region. The rocks are grouped into the Sobreiro and Santa Rosa formations, which are not metamorphosed and are less modified by weathering processes (Silva et al., 2014; Cruz et al., 2014). In this region, areas of artisanal mining of cassiterite and monazite occupy large areas in open pits. The main methods used to extract cassiterite and monazite in the region include open-pit exploration with mechanical dismantling and the use of machines, generating material classified as sterile; afterwards, hydraulic dismantling is carried out, generating a mud-like material that is later processed. The processing method is carried out by using the jigging process, separating ore from the waste. Both waste and tailings are deposited in piles in the explored areas.

The sampling areas were identified as: OV1 = active mine waste (10 samples); TA1 = active mine tailings (8 samples); OV2 = waste from mines deactivated one year ago (4 samples); TA2 = tailings from mines that were deactivated one year ago (3 samples); OV3 = waste from mines that were deactivated ten years ago (4 samples); TA3

= tailings from mines that were deactivated 10 years ago (3 samples); and RA = natural forest soil (3 samples), considered as reference, totalized 35 samples (Fig. 1, Table 1S).

### Fig. 1.

Artisanal mining areas of monazite and cassiterite in the municipality of São Félix do Xingu, southeastern Brazilian Amazon.



In each area, five single samples (separated by 50 m) were collected to form a composite, using a dutch stainless steel auger. For each composite sample, approximately 2.5 kg of material was collected from a depth of 0.0 to 0.2 m. After collection, the materials were sieved at 2 mm, air-dried and stored in polyethylene bags until analysis.

## **2.2. Chemical Characterization of samples**

The chemical properties and particle size of soils and mining waste were determined according to (Teixeira et al., 2017). The pH was determined in H<sub>2</sub>O using a potentiometer and quantified using a meter at a soil-water ratio of 1:2.5, pHmetro Thermo Scientific equipment.. Exchangeable concentrations of calcium (Ca<sup>2+</sup>) and magnesium (Mg<sup>2+</sup>) were extracted using 1 mol L<sup>-1</sup> KCl and quantified by atomic absorption spectrophotometry. The available concentration of P and K were extracted with Mehlich-1, and determined by colorimetry (P) and flame photometry (K). The effective cation exchange capacity (CEC) was obtained from the sum of the exchangeable concentrations of Ca<sup>2+</sup>, Mg<sup>2+</sup>, K<sup>+</sup> and Al<sup>+3</sup>. The organic carbon content was determined by wet combustion with potassium dichromate and multiplied by 1.72 to determine the organic matter (OM) content. Soil texture was determined by the pipette method (Gee and Bauder, 1986).

## **2.3 Pseudo total concentrations of rare earth elements**

Total concentrations of REEs were extracted in triplicate using the alkaline fusion method described by (Pereira et al., 2023), and quantified by inductively coupled plasma mass spectrometry (ICP-MS, PerkinElmer). Fe concentrations in the extracts were also quantified by ICP-MS to calculate pollution indices. For analytical quality control, blank samples and certified reference material (GRE-3®) were included in each analytical batch. Recovery rates varied between 63.1 and 95.2% (Table 2S).

The geochemical signatures of the REEs were obtained from geochemical normalization considering the ratios between the concentration observed in the study and the concentration described by Rudnick and Fountain (1995) for the continental crust, considering that these values are more appropriate for the characteristics of the Amazon

(Ferreira et al., 2021; Pereira et al., 2023). REEs were grouped into light (LREEs – Ce, Nd, La, Pr, Sm and Eu) and heavy (HREEs – Y, Gd, Dy, Er, Yb, Ho, Tb, Lu and Tm), based on atomic mass (Galhardi et al., 2020; Li et al., 2020), and the  $\sum$ LREE/ $\sum$ HREE ratio was calculated to elucidate the fractionation of the elements (Fernández-Caliani and Grantcharova, 2021; Medas et al., 2013).

## 2.4 Pollution assessment

The REEs contamination levels were evaluated based on the contamination factor (CF), enrichment factor (EF) and the pollutant load index (PLI) (Khan et al., 2020; Sergeeva et al., 2021; Zerizghi et al., 2023). For the calculations, RA was considered as a reference for the natural environment, due to the low or absent impact of mining activities in this area, as suggested by previous studies (Araújo et al., 2021; Covre et al., 2022; Pereira et al., 2020; Souza Neto et al., 2020).

CF is an index that is frequently used to assess the level of pollution associated with REEs in areas altered by mining (Godwyn-Paulson et al., 2022; Jiménez-Ballesta et al., 2022; Wang et al., 2022), obtained from according to Eq. (1):

$$CF = \frac{C_{REE}}{B_{REE}}$$

(1)

where CREE is the average REE concentration ( $\text{mg kg}^{-1}$ ) in the altered area and BREE is the concentration of the same REE in RA. CF values were interpreted as follows:  $CF < 1$  indicates low contamination,  $CF$  between  $1 - 3$  indicates moderate contamination,  $CF$  between  $3 - 6$  indicates considerable contamination, and  $CF > 6$  indicates high contamination (Hakanson, 1980).

The EF was calculated to identify the level of enrichment associated with REEs (Azizi et al., 2022; Saleh et al., 2022; Zerizghi et al., 2023), according to Eq. (2):

$$EF = \left( \frac{C_{REE}}{C_{Fe}} / \frac{B_{REE}}{B_{Fe}} \right) \quad (2)$$

where CTR is the REE concentration in the sample, CFe is the Fe concentration in the same sample ( $\text{mg kg}^{-1}$ ), BREE is the REE concentration in RA, and BFe is the Fe concentration in RA. Fe was used for geochemical normalization due to its conservative behavior (Pereira et al., 2022). EF values were interpreted as follows:  $EF < 2$  indicates minimal enrichment, EF between 2 – 5 indicates moderate enrichment, EF between 5 – 20 indicates significant enrichment, EF between 20 – 40 indicates high enrichment, and  $EF > 40$  indicates enrichment extreme (Sutherland, 2000).

The PLI is a widely used measure to estimate cumulative REE pollution (Abbasi et al., 2021; Jean-Lavenir et al., 2023; Sojka et al., 2021), obtained according to Eq. (3):

$$PLI = (CF_1 \times CF_2 \times CF_3 \times \dots \times CF_n)^{1/n} \quad (3)$$

where CF is the contamination factor and n is the number of REEs under study. PLI values were classified into two levels: PLI ranging from 0 to 1 indicates no pollution and  $PLI > 1$  indicates polluted material (Tomlinson et al., 1980).

## 2.5 Environmental risk assessment

The potential ecological risk factor (PERF) and the potential ecological risk index (PERI) were calculated to evaluate the impacts of REEs to the ecosystem in the studied areas ( Liu et al., 2023; Pereira et al., 2023; Saha et al., 2023). PERF makes it possible

to understand the individual ecological risks of REEs in areas altered by mining. In this study, EF was incorporated into the PERF calculation (Kumar et al., 2020; Lima et al., 2022), according to Eq. (4):

$$PERF_{REE} = EF_{REE} \times TRF_{REE} \quad (4)$$

where EFREE is the REE enrichment factor and TRFREE is the REE toxicity response factor. The results were interpreted as follows:  $PERF < 40$  indicates low risk,  $PERF$  between  $40 - 80$  indicates moderate risk,  $PERF$  between  $80 - 160$  indicates considerable risk,  $PERF$  between  $160 - 320$  indicates high risk, and  $PERF > 320$  indicates very high risk (Hakanson, 1980).

The PERI allows us to know the effects of the joint action of REEs on the ecosystem (Chen et al., 2020; Wang et al., 2021; Wu et al., 2019b), found according to Eq. (5):

$$PERI = PERF_1 + PERF_2 + PERF_3 + \dots + PERF_n \quad (5)$$

where  $PERF$  is the potential ecological risk factor and  $n$  is the number of elements under study. PERI values were interpreted as follows:  $PERI < 150$  indicates low risk,  $PERI$  between  $150 - 300$  indicates moderate risk,  $PERI$  between  $300 - 600$  indicates considerable risk, and  $PERI > 600$  indicates very high risk (Hakanson, 1980).

## **2.6 Human health risk assessment**

Health risk assessment is essential for estimating potential carcinogenic and non-carcinogenic risks depending on three possible routes of contamination, which can be: dermal, oral or pulmonary in possible exposure to contaminated material (Fig. 2) (Pereira et al., 2021; Pereira et al., 2022; Souza Neto., 2020; Covre et al., 2021). There are no specific values in the literature for risk assessment for REEs, however, the estimate is made considering SF  $3.2 \times 10^{-12}$  for the group of elements (Ferreira et al, 2022).

The non-carcinogenic potential risk to human health was based on the average daily dose (ADD), considering three routes: ingestion (ADD<sub>ing</sub>), inhalation (ADD<sub>inh</sub>) and dermal contact (ADD<sub>der</sub>). The hazard quotient (HQ) and risk index (HI) were calculated for adults and children. To find the potential carcinogenic risk, the ADD was multiplied by the slope factor (SF) to produce a cancer risk level (Eq. 6-12):

$$ADD_{ing} = C \times \left( \frac{R_{ing} \times EF \times ED}{BW \times AT} \right) \times CF \quad (6)$$

$$ADD_{inh} = C \times \left( \frac{R_{inh} \times EF \times ED}{PEF \times BW \times AT} \right) \times CF \quad (7)$$

$$ADD_{der} = C \times \left( \frac{SL \times SA \times ABS \times EF \times ED}{BW \times AT} \right) \times CF \quad (8)$$

$$HQ_{ing} = ADD_{ing}/Rfd \quad (9)$$

$$HQ_{inh} = ADD_{inh}/Rfd \quad (10)$$

$$HQ_{der} = ADD_{der}/Rfd \quad (11)$$

$$HI = \sum HQ \quad (12)$$

where ADD ( $\text{mg kg}^{-1} \text{ d}^{-1}$ ) is the average daily dose ( $\text{mg kg d}^{-1}$ ; C is the REE concentration of REE ( $\text{mg kg}^{-1}$ ); Ring is the intake rate,  $100 \text{ mg d}^{-1}$  for adults and  $200 \text{ mg d}^{-1}$  for children (USEPA, 2001); Rinh is the inhalation rate,  $7.6 \text{ m}^3 \text{ day}^{-1}$  for children

and  $20 \text{ m}^3 \text{ day}^{-1}$  for adults (Lu et al., 2014; USEPA, 2001); PEF is the particle emission factor,  $1.36 \times 10^9 \text{ m}^3 \text{ kg}^{-1}$  (USEPA, 2001); SL is the skin adherence factor,  $0.2 \text{ cm}^{-2} \text{ d}^{-1}$  for children and  $0.875 \text{ cm}^{-2} \text{ d}^{-1}$  for adults (USEPA, 2001); SA is area of exposed skin,  $732 \text{ cm}^2$  for children and  $3202 \text{ cm}^2$  for adults (USEPA, 2001); ABS is the dermal absorption factor, 0.03 (Lu et al., 2014); EF is the exposure frequency,  $279 \text{ d y}^{-1}$  (Moreira et al., 2018); ED is the duration of exposure, 24 y for adults and 4 y for children (Moreira et al., 2018); BW is body weight, 70 kg for adults and 16 kg for children (Moreira et al., 2018); AT is the average time, with no carcinogenic effects ( $\text{ED} \times 365 \text{ d}$ ) and carcinogenic effects ( $70 \text{ y} \times 365 \text{ d}$ ); CF is the conversion factor,  $10^{-6} \text{ kg mg}^{-1}$  (USEPA, 2001); Rfd is the reference dose) (USEPA, 2001); and SF is the slope factor for all REEs,  $3.2 \times 10^{-12}$  (Sun et al., 2017).

## 2.7 Statistical analyzes

The results were submitted to descriptive statistical analysis and data normality was tested using the Shapiro-Wilk test ( $p < 0.05$ ). Data that did not present a normal distribution were subjected to logarithmic transformation. After data normalization, a Pearson correlation analysis and principal component analysis (PCA) were performed to understand the relationship between REEs concentrations and material properties. All analyzes were performed using R software version 4.3.1 (R Core Team, 2023).

### 3. RESULTS AND DISCUSSIONS

#### 3.1. Chemical properties and particle size distribution

The pH values ranged from 4.5 to 4.87 (Table 1), indicate high acidity in the areas studied (Venegas et al., 1999). The acidity found in the reference area is within the pH range commonly observed for natural soils in the Amazon (Souza et al., 2018). In this region, intense climatic conditions promote the erosion of primary minerals and a reduction in soil pH (Quesada et al., 2020). The acidity observed in mining waste, in turn, can be explained by the oxidation of sulfides exposed to atmospheric conditions, which decreases the pH over time (Azizi et al., 2022), as well as by the intense leaching of bases and permanence of H<sup>+</sup> and Al<sup>+3</sup> ions (Chen et al., 2023).

**Table 1.**

Chemical properties and granulometry of soils and mining residues in the studied areas.

Areas	Properties					
	pH (in water)	OM (g dm <sup>-3</sup> )	CEC (cmol <sub>c</sub> dm <sup>-3</sup> )	Clay g	Sand	Silt
OV1	4.5 ± 0.1	28.2 ± 5.7	1.9 ± 0.6	21.5 ± 6.7	68.1 ± 10.8	10.4 ± 10.2
TA1	4.5 ± 0.2	11.7 ± 8.3	0.8 ± 0.3	11.2 ± 8.6	81.6 ± 14.3	7.2 ± 6.4
OV2	4.5 ± 0.2	40.8 ± 3.8	1.4 ± 0.3	30.2 ± 7.9	63 ± 9.5	6.8 ± 3.0
TA2	4.7 ± 0.2	9.3 ± 0.4	0.8 ± 0.1	16.5 ± 2.6	72.2 ± 7.7	11.3 ± 5.7
OV3	4.7 ± 0.3	37.7 ± 1.3	1.7 ± 0.4	46.3 ± 2.9	44.1 ± 1.5	9.6 ± 4.4
TA3	4.9 ± 0.1	13.6 ± 2.9	0.7 ± 0.3	21.2 ± 3.3	68.1 ± 4.9	10.8 ± 4.6
RA	4.9 ± 0.1	57.7 ± 3.4	2.3 ± 0.1	44.4 ± 0.4	41 ± 0.5	14.5 ± 0.2

OM = Organic matter; CEC = Cation exchange capacity.

The OM levels about six times lower in anthropized areas compared to the reference area (Table 1). These results are related to scarce vegetation cover and low deposition of organic residues in the surface layer, unlike the soil in the reference area, which has dense forest, with large trees (Alarcón-Aguirre et al., 2023; Liu et al. , 2021). In waste rock and tailings areas, the lower OM levels can also be explained by the predominantly mineral composition of these materials. Tailings are made up of rocks processed in mineral processing, while waste rock is made up of soils (which normally contain OM) and rocks of no commercial interest for mining (Chileshe et al., 2020; Nwaila et al., 2021).

The CEC had results in the order RA > OV1 > OV3 > OV2 > TA1 = TA2 > TA3, with values up to 65% higher in the reference area, when compared to the impacted areas. According to the classification by Venegas et al. (1999), CEC was low in the reference area and very low in areas altered by mining. The low CEC evidenced in the reference area is related to the predominant mineralogy of the region's soils, which include Fe and Al oxides, with a low natural capacity to retain cations (Souza et al., 2018). The even lower CEC in mining waste can be explained by lower OM contents, which is fundamental for CEC in tropical regions (Mabagala and Mng'ong'o, 2022; Ramos et al., 2018; Souza et al., 2018). Lower CEC values were also observed in artisanal Au mining areas in the southeast and northeast of the Brazilian Amazon (Pereira et al., 2023, 2022).

The clay contents followed the order: reference area > waste > tailings, which also contributes to a higher CEC in the areas of waste deposition in relation to tailings (Table 1), given the contribution of the clay fraction to the chemical activity of the medium. (Enang et al., 2022). Sand contents ranged from 44.1 to 81.6% in mining waste and were equal to 41% in the soil of the reference area, indicating coarser grain size in the altered areas. Furthermore, mining tailings had coarser particle sizes than waste rock, suggesting

unfavorable conditions for the formation of aggregates (Chileshe et al., 2020), which was evidenced by the lower OM contents in the tailings. Such conditions indicate greater difficulty in revegetating altered areas and, therefore, measures are necessary to improve the chemical and physical properties of the environment and favor environmental rehabilitation (Gastauer et al., 2020).

### **3.2. Concentrations, fractionation and geochemical signatures of REEs**

All REEs had higher concentrations in areas altered by mining when compared to the reference area, especially Tb, Tm, Y and Sc in TA2 tailings, which had results 73.3 to 769 times higher (Table 2). Ce had the highest concentrations, regardless of the area evaluated. High concentrations of Ce were already expected in this study, considering that this element is the REE found in the highest levels in soils worldwide (Jiménez-Reyes et al., 2021; Su et al., 2021). Similar results were observed in artisanal Au mines in the eastern Amazon (Pereira et al., 2023, 2022).

The tailings had higher concentration trends than the waste, especially Tm and Yb in TA2, with results respectively 128 and 27 times higher in the waste than in the waste (Table 2). Furthermore,  $\Sigma$ REE values were 512% higher in TA1 than in OV1, 148% higher in TA2 than in OV2, and 139% higher in TA3 than in OV3, reinforcing the greater accumulations of REEs in mining tailings. These results can be explained by the greater richness of REEs in rocks processed in mineral processing (Azizi et al., 2022), and suggest that REE extraction methods may be showing low efficiency in the artisanal mines studied.

TA2 waste had the highest concentrations of all REEs studied, with the exception of Y (Table 2). These materials come from the mineral processing of trachyandesite-type rocks, which have a wealth of minerals such as apatite, naturally enriched by REEs, mainly LREEs (J. Liu et al., 2023). The replacement of Ca+2 by REEs promotes the enrichment of these elements in apatite (Banihashemi et al., 2019; Soltani et al., 2019). Depending on the techniques adopted in processing, mining tailings may present high concentrations of REEs (Pyrgaki et al., 2021), which was evidenced in TA2 tailings.

**Table 2.**

Concentrations of REEs in the studied areas.

Element ( $\text{mg kg}^{-1}$ )	Areas				
	OV1	TA1	OV2	TA2	OV3
Ce	$42.4 \pm 50$	$240.1 \pm 543.5$	$433.1 \pm 674.0$	$516.9 \pm 841.5$	$46.9 \pm 49.8$
Dy	$3.1 \pm 2.4$	$11.6 \pm 23.7$	$12.8 \pm 17.2$	$23.5 \pm 37.5$	$2.5 \pm 2.1$
Er	$2.6 \pm 1.8$	$8.3 \pm 16.3$	$7.8 \pm 9.4$	$16.3 \pm 25.5$	$2.0 \pm 1.5$
Eu	$0.1 \pm 0.0$	$0.3 \pm 0.4$	$0.3 \pm 0.4$	$0.5 \pm 0.7$	$0.1 \pm 0.1$
Gd	$2.3 \pm 1.8$	$10.4 \pm 22.2$	$14.8 \pm 22.1$	$21.5 \pm 34.9$	$2.0 \pm 2.0$
Ho	$0.7 \pm 0.5$	$2.5 \pm 5.0$	$2.5 \pm 3.2$	$5.0 \pm 7.9$	$0.6 \pm 0.4$
La	$19.3 \pm 13.5$	$121.8 \pm 287.6$	$230.4 \pm 360.2$	$271.9 \pm 447.0$	$22.8 \pm 20.3$
Lu	$0.5 \pm 0.4$	$1.5 \pm 2.8$	$1.4 \pm 1.5$	$2.9 \pm 4.4$	$0.4 \pm 0.3$
Nd	$12.4 \pm 9.3$	$77.3 \pm 180.7$	$139.1 \pm 218.3$	$162.5 \pm 265.6$	$13.5 \pm 13.3$
Pr	$3.9 \pm 2.8$	$24.4 \pm 57.7$	$44.0 \pm 69.0$	$52.9 \pm 86.6$	$4.4 \pm 4.2$
Sc	$1.2 \pm 1.0$	$6.9 \pm 4.9$	$2.36 \pm 2.5$	$19.1 \pm 4.0$	$2.2 \pm 2.4$
Sm	$2.4 \pm 1.9$	$12.8 \pm 28.6$	$22.0 \pm 34.1$	$27.2 \pm 44.4$	$2.4 \pm 0.4$
Tb	$0.5 \pm 0.4$	$1.8 \pm 3.7$	$2.0 \pm 3.1$	$15.4 \pm 5.9$	$0.4 \pm 22.5$
Tm	$0.4 \pm 0.3$	$1.3 \pm 2.6$	$1.2 \pm 1.4$	$153.8 \pm 3.9$	$0.3 \pm 0.2$
Y	$23 \pm 18$	$75.2 \pm 148.0$	$72.9 \pm 91.6$	$21.8 \pm 244.9$	$17.4 \pm 14.3$
Yb	$3.5 \pm 2.4$	$9.8 \pm 18.3$	$5.70 \pm 10.2$	$154.0 \pm 29.1$	$2.7 \pm 1.8$
$\sum \text{REE}$	118.3	606.0	992.4	1465.2	120.6
$\sum \text{LREE}$	80.5	476.7	868.9	1031.9	90.1
$\sum \text{HREE}$	36.6	122.4	121.1	414.2	28.3
$\sum \text{LREE}/\sum \text{HREE}$	2.2	3.9	7.2	2.5	3.2

On the other hand, OV3 and TA3 are among the three areas with the lowest concentrations of all REEs studied, except Eu and Sc (Table 2). In these areas, it is likely that the longer exposure to intense weathering in Amazonian conditions is directly contributing to the reduction in REEs concentrations (Ferreira et al., 2021). Previous studies carried out in the northeast of the Brazilian Amazon indicated that the longer exposure time of waste directly contributes to reducing the concentrations of toxic

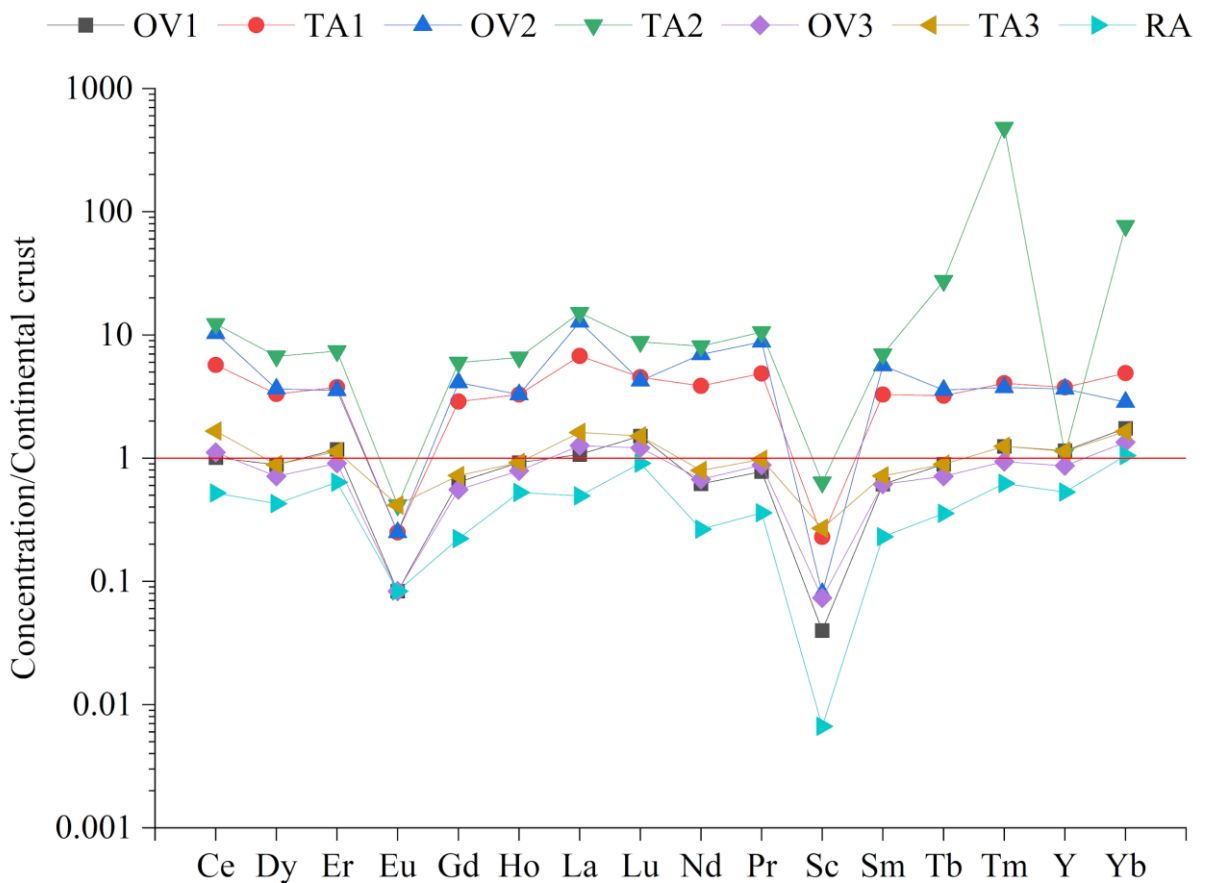
elements such as arsenic (As) (Souza Neto et al., 2020) and mercury (Hg) (Teixeira et al., 2021).

The  $\sum$ LREE were higher than  $\sum$ HREE in all areas studied, with  $\sum$ LREE/ $\sum$ HREE ranging from 2.2 (RA) to 7.2 (A3) (Table 2). Although the RA had  $\sum$ LREE/ $\sum$ HREE above 1, this ratio was higher in the altered areas, with the exception of OV1, which had  $\sum$ LREE/ $\sum$ HREE similar to the reference area. These results suggest that artisanal activities favor greater accumulation of LREEs in relation to HREEs, which may be directly related to the natural occurrence of LREEs in the areas studied (Cruz et al., 2014; Ferreira and Lamarão, 2013). Furthermore, both  $\sum$ LREE and  $\sum$ HREE were higher in tailings deposition areas, which reinforces the greater richness of REEs in mineral processing waste and the greater attention that should be directed to these materials.

The geochemical signatures show that there are positive anomalies ( $>1$ ) for Ce, Dy, Er, Gd, Ho, La, Lu, Nd, Pr, Sm, Tb, Tm, Y and Yb in TA1, OV2 and TA2; Ce, La, Lu and Yb in OV1, Ce, La, Lu and Vb in OV3; Ce, Er, La, Lu, Tm, Y and Yb in TA3. Eu and Sc showed negative signatures in all areas and materials studied (Fig. 3), based on continental crust values (Rudnick and Fountain, 1995).

**Fig. 3.**

Geochemical signatures of REEs in the studied areas.



RA: Reference área.

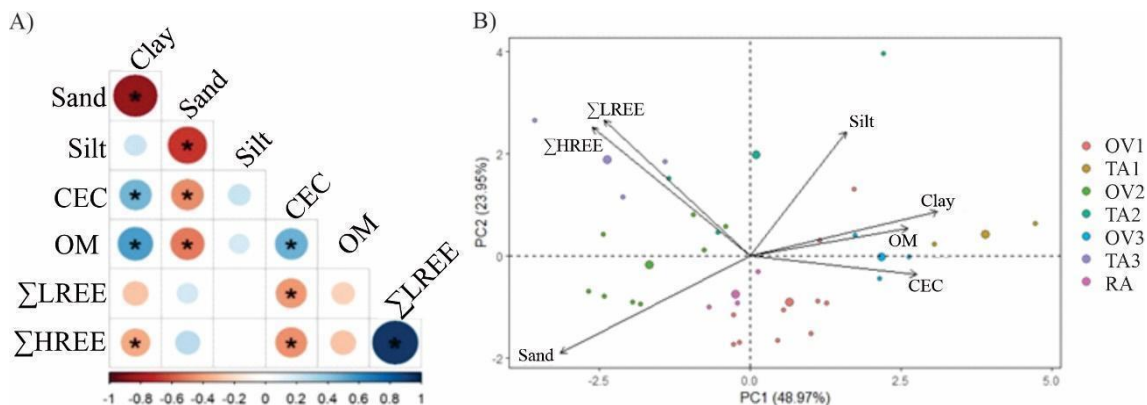
Areas disturbed by artisanal mining accumulated LREEs and HREE in active mining areas (tailings) and those deactivated a year ago underground (tailings and waste). Greater accumulation of LREEs was found by Pereira et al. (2023) in gold mining areas in the Amazon. Due to the sandier particle size of the tailings (Table 1), these residues deserve special attention, as they have a low potential for cation retention, which favors the leaching of REEs (Feitosa et al., 2020; Padoan et al., 2021). Furthermore, the low pH of waste rock and tailings favors the release of bioavailable concentrations of REEs, which can increase risks to the ecosystem and human health (Costis et al., 2021; Ou et al., 2022).

### 3.3. Relationship between variables

Significant Pearson correlation coefficients ( $p < 0.05$ ) were observed between REEs and soil properties (Fig. 4, Table 3S). Positive correlations were observed between  $\sum\text{LREE}$  and  $\sum\text{LREE}$  (0.94), suggesting similar geochemical sources and behavior for these groups of elements (Lima et al., 2022; Pereira et al., 2023), as well as between CEC and OM (0.94), 48), which reinforces the role of OM for CEC in the areas studied (Ferreira et al., 2021). Otherwise, negative and significant correlations were observed between  $\sum\text{LREE}$  and CEC (-0.43), and between  $\sum\text{HREE}$  and clay (-0.38) and CEC (-0.45). These results can be explained by the lower levels of clay, OM and CEC observed in areas altered by mining, which had higher concentrations of REEs, arising from the mobilization of rocks rich in these elements (Table 2).

**Fig. 4.**

Pearson correlation analysis (A) and principal component analysis (B) between sample properties and concentrations of REEs in the studied areas.



Principal component analysis allowed explaining 72.92% of the total data variability, with 48.97% explained by PC1 and 23.95% by PC2 (Fig. 4). High loads and a strong relationship were observed for clay (0.8), CEC (0.73), and OM (0.7), which can be explained by the greater chemical activity of the clay fraction and OM, which generate

negative charges for the cation retention (Bi et al., 2023; Liu et al., 2020). Furthermore, a strong relationship was evidenced between  $\sum$ LREEs and  $\sum$ HREEs, which reinforces the similar behavior and origin of these elements.

### **3.4. Pollution índices**

The CF values indicated contamination ranging from moderate to very high (Table 3), that is, all areas altered by mining present contamination by REEs (Hakanson, 1980). The elements Ce, Dy, Er, Ho, La, Lu, Nd, Pr, Tb, Tm, Y and Yb had moderate contamination, regardless of the area studied. Considerable contamination was evident for Eu in all areas except OV1, as well as for Gd and Sm in OV2, TA2 and OV3. The element with the highest CF was Sc, whose contamination level was classified as very high in all areas studied. Based on the PLI results, which ranged from 2.3 to 2.9, it is possible to state that all areas are polluted by the multiple effects of REEs (PLI > 1.0).

**Table 3.**

Contamination factor (CF), enrichment factor (EF), and pollution load index (PLI) of rare earth elements.

Element	OV1		TA1		OV2		TA2		OV3
	CF	EF	CF	EF	CF	EF	CF	EF	CF
Ce	1.9 ± 1.2	2.0 ± 1.4	2.0 ± 24.8	3.5 ± 5.7	2.3 ± 30.7	10.9 ± 6.9	2.4 ± 38.3	15.5 ± 9.0	2.4 ± 1.1
Dy	2.1 ± 1.6	2.2 ± 1.5	2.2 ± 16.2	2.2 ± 3.9	2.5 ± 11.7	4.9 ± 2.2	2.5 ± 25.6	10.7 ± 5.7	2.5 ± 1.1
Er	1.9 ± 1.3	2.0 ± 1.2	1.9 ± 12.0	2.1 ± 2.9	2.1 ± 7.0	3.3 ± 1.1	2.2 ± 18.8	8.3 ± 3.9	2.1 ± 1.1
Eu	2.6 ± 1.6	2.2 ± 0.9	3.3 ± 10.3	2.6 ± 1.2	3.7 ± 12.6	4.3 ± 1.3	4.4 ± 20.7	10.5 ± 2.4	4.3 ± 1.1
Gd	2.9 ± 2.3	2.5 ± 2.7	2.9 ± 27.9	3.6 ± 8.1	3.4 ± 27.8	8.8 ± 7.4	3.5 ± 43.9	15.4 ± 12.7	3.4 ± 2.2
Ho	1.9 ± 1.4	2.1 ± 1.2	1.9 ± 13.0	2.2 ± 3.0	2.1 ± 8.4	3.8 ± 1.4	2.2 ± 20.4	9.0 ± 4.3	2.1 ± 1.1
La	2.2 ± 1.5	2.2 ± 1.6	2.2 ± 32.1	4.3 ± 7.5	2.5 ± 40.3	14.1 ± 9.1	2.5 ± 49.9	19.8 ± 12.1	2.5 ± 1.1
Lu	1.6 ± 1.1	1.6 ± 1.8	1.6 ± 8.3	1.5 ± 2.2	1.8 ± 4.6	2.3 ± 0.7	1.8 ± 13.1	5.7 ± 2.7	1.8 ± 0.8
Nd	2.3 ± 1.8	2.3 ± 1.9	2.4 ± 34.1	4.5 ± 8.3	2.8 ± 41.2	13.8 ± 9.8	2.8 ± 50.1	19.3 ± 12.6	2.8 ± 2.2
Pr	2.1 ± 1.5	2.1 ± 1.6	2.1 ± 30.9	4.2 ± 7.1	2.4 ± 36.9	12.9 ± 8.3	2.5 ± 46.3	18.5 ± 11.1	2.5 ± 1.1
Sc	6.4 ± 5.4	4.3 ± 2.3	13.3 ± 25.6	7.7 ± 2.2	14.2 ± 13.4	4.5 ± 1.4	20.5 ± 21.3	43.4 ± 3.3	20.3 ± 8.9
Sm	2.7 ± 2.1	2.5 ± 2.5	2.8 ± 31.7	4.1 ± 8.6	3.3 ± 37.9	12.0 ± 9.9	3.3 ± 49.3	17.8 ± 13.6	3.3 ± 2.2
Tb	2.4 ± 1.9	2.5 ± 1.8	2.4 ± 19.4	3.1 ± 4.6	2.8 ± 16.2	6.5 ± 3.2	2.9 ± 31.1	12.9 ± 7.1	2.8 ± 1.1
Tm	1.8 ± 1.3	1.9 ± 1.1	1.8 ± 10.3	1.8 ± 2.4	2.0 ± 5.7	2.9 ± 0.8	2.0 ± 15.7	7.2 ± 3.1	2.0 ± 0.8
Y	2.2 ± 1.7	2.3 ± 1.5	2.1 ± 13.9	2.4 ± 3.4	2.4 ± 8.6	3.9 ± 1.4	2.5 ± 23.0	9.9 ± 5.0	2.4 ± 1.1
Yb	1.6 ± 1.1	1.8 ± 1.0	1.6 ± 8.5	1.6 ± 2.1	1.8 ± 4.7	1.6 ± 0.7	1.8 ± 13.5	6.2 ± 2.6	1.8 ± 0.8
PLI	2.3		2.4		2.8		2.9		2.9

The EF values revealed that areas OV1, TA1, OV3 and TA3 have enrichment ranging from absent to moderate for all REEs, except Sc in TA1, OV3 and TA3, with significant enrichment (Table 3). On the other hand, areas OV2 and TA2 had a greater number of REEs with high levels of enrichment, especially TA2, which showed significant enrichment for all REEs, with the exception of Sc, which had extreme enrichment (Sutherland, 2000). EF results above 1.5, which indicate predominantly anthropogenic origin (Mîndrescu et al., 2022; Mor et al., 2022), were evidenced for all elements in OV1, TA1, OV2, TA2 and OV3 (except Eu ), and only for Eu and Sc in TA3.

Areas OV3 and TA3 have lower levels of contamination and enrichment by REEs, which can be explained by the longer exposure time of residues on the soil surface. In these areas, high precipitation levels may be directly contributing to the removal of REEs through leaching and surface runoff (de Lima et al., 2022; Velásquez Ramírez et al., 2020), especially in TA3, which had low CEC (Table 1). Although these materials have shown lower levels of contamination, environmental monitoring is necessary to mitigate the spread of contaminants to areas influenced by artisanal mining.

The contamination rates reinforce that waste and tailings with one year of deposition (OV2 and TA2) show a greater accumulation of REEs. Among all the materials evaluated, TA2 presents the highest levels of contamination and enrichment of all REEs, indicating that rock processing is accumulating high levels of these elements in the surface layer of the soil. Therefore, OV2 and especially TA2 demand special attention due to the potential risks they can cause to the ecosystem and human health (Galhardi et al., 2020; Wang et al., 2022). Measures must be implemented to mitigate the accumulation of these wastes inappropriately in the environment, considering the greater wealth of REEs in the rocks explored in these areas.

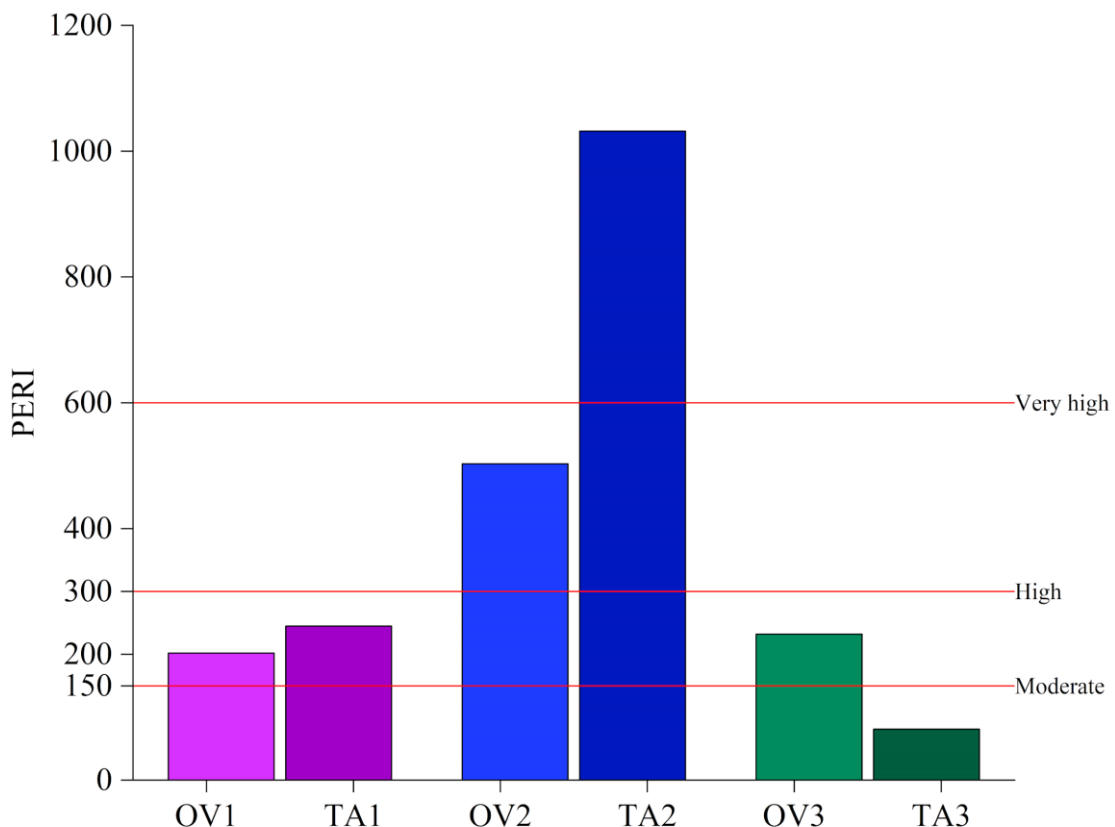
### **3.5. Environmental risks**

PERF values were varied for the REEs and areas studied (Table 4S). All elements had PERF classified as low in OV1, TA1, OV3 and TA3, with the exception of Lu in OV3, which was classified as moderate (Hakanson, 1980). On the other hand, OV2 and TA2 had higher PERF values, ranging from low (Ce, Dy, Er, Ho, La, Nd, Tm, Y, Yb and Sc) to moderate (Eu, Gd, Lu, Pr, Sm and Tb) in OV2, and classified as low for Ce, La, Nd, Y and Yb, moderate for Dy, Er, Gd, Tm and Sc, and considerable for Eu, Ho, Lu, Pr, Sm and Tb in TA2.

The PERI results, which allow us to know the impacts of the associated effect of REEs, were low in TA3, moderate in OV1, TA1 and OV3, moderate in OV3, high in OV2 and very high in TA2 (Fig. 5). These results indicate lower impacts on the ecosystem in TA3, which can be explained by the longer exposure time of materials on the soil surface. On the other hand, areas OV2 and especially TA2 can pose a serious threat to the ecosystem. La and Ce can deform and inhibit the extension of roots and aerial parts of plants (Oliveira et al., 2015). Yttrium has a negative effect on the percentage and speed of germination of native and edible species (Thomas et al., 2014). In onion bulbs, *Allium cepa L*, moistened with aqueous solutions of La and Ce chloride in spodosol samples, a significant reduction in the mitotic index was observed at all tested concentrations of La and Ce. The frequency of cells with deformity increased significantly by 50 mg L<sup>-1</sup> after exposure to the tested REE (Kotelnikova et al., 2019).

**Fig. 5.**

Potential ecological risk indices of REEs.



The level of anthropization of the environment contributes to the increase in the concentration of REEs, mainly due to the reduction in OM and mechanical breakdown of the material. This can promote high ecological risks for the environment due to multiple exposure to contaminants. Active and recently deactivated areas represent a great ecological risk due to high concentrations of REE, making it necessary to take mitigating measures.

### 3.6. Human health risks

In the study region there is a high risk of contact with the population, which can occur via inhalation due to dust and inadequate disposal of material near dirt roads, which exposes residents to material with a high concentration of REEs. It is worth mentioning that the mined areas are physically close to the urban area, which can represent an aggravating factor in exposure to contaminated material. Furthermore, workers in artisanal areas are susceptible to inhalation, dermal contact and accidental ingestion of material rich in REEs (Souza Neto et al, 2020; Souza et al., 2017).

The results of "HQcrianças" presented mean values ranging from  $6.7 \times 10^{-5}$  (Eu in OV3) to  $1.1 \times 10^{-2}$  (La and Ce, for sterile in OV2 and TA1, respectively), while the mean values of HQ adults ranged from  $9.4 \times 10^{-5}$  (Tb, for tailings in TA1) to  $1.3 \times 10^{-2}$  (Ce and La, for TA2 and tailings in OV1, respectively) (Table 4).

**Table 4.**

Risk indices for adults and children from exposure to REEs in the studied areas.

Risks	Areas	Group	
		Adults	Children
Non-carcinogenic	OV1	$6.5 \times 10^{-3}$	$5.7 \times 10^{-2}$
	TA1	$3.2 \times 10^{-2}$	$2.8 \times 10^{-1}$
	OV2	$5.4 \times 10^{-2}$	$4.8 \times 10^{-1}$
	TA2	$7.0 \times 10^{-2}$	$6.1 \times 10^{-1}$
	OV3	$6.6 \times 10^{-3}$	$5.8 \times 10^{-2}$
	TA3	$9.1 \times 10^{-3}$	$8.0 \times 10^{-2}$
Carcinogenic	OV1	$2.2 \times 10^{-16}$	$1.9 \times 10^{-15}$
	TA1	$1.1 \times 10^{-15}$	$9.5 \times 10^{-15}$
	OV2	$1.8 \times 10^{-15}$	$1.6 \times 10^{-14}$
	TA2	$2.3 \times 10^{-15}$	$2.0 \times 10^{-14}$
	OV3	$2.2 \times 10^{-16}$	$1.9 \times 10^{-15}$
	TA3	$3.0 \times 10^{-16}$	$2.7 \times 10^{-15}$

The HI values obtained were less than 1 for children and adults, indicating low non-carcinogenic and carcinogenic risk from exposure to REEs (USEPA, 2004).

In this study, carcinogenic risks were considered low, however the high concentrations of La and Ce may justify concern about the carcinogenic risk, mainly because gaps regarding the carcinogenic risk of this group of elements still need to be elucidated. High concentrations of La and Ce are related to oral carcinogenic risks (Chen et al., 2022; He et al., 2021) and associated with patients with brain tumors (Gaman et al., 2021).

The absence of contamination risks observed in this study is in line with previous results for Amazonian soils (Ferreira et al., 2021). These authors observed that the human health risk due to REEs contamination was considered low in Amazonian soils, although they observed enrichment in the concentrations of these elements. Human exposure to REEs occurs through ingestion of contaminated food and water, inhalation, and dermal contact. Further investigations are needed regarding the routes of exposure and carcinogenic or non-carcinogenic effects and consequently risks to human health promoted by the accumulation of REEs in areas subjected to artisanal exploitation of cassiterite and monazite. (Gwenzi et al., 2018).

#### **4. CONCLUSIONS**

The artisanal exploration of monazite and cassiterite caused an increase in concentrations, high enrichment and a high contamination factor by REEs. Active and recently deactivated mines presented higher concentrations of Ce, La, Nd and Y, and high ecological risk, while the other areas presented moderate potential ecological risk. The health risk to children and adults was low. The results presented in this study, as well as its conclusions, demonstrate to those responsible for public environmental protection policies and environmentalists, the need to remediate areas affected by mining,

immediately and simultaneously with exploration, to reduce environmental contamination and prevent health risks due to high concentrations of REEs, on site and in areas potentially influenced by mining. It is also necessary to expand studies involving absorption dynamics and risks for REEs, the existence of a single slopp factor for all elements may underestimate or overestimate health risk assessment values.

Determining the bioavailability and bioaccessibility, in addition to the chemical forms of occurrence of REEs, is necessary to better understand the dynamics and real risk to human and environmental health of these elements.

## REFERENCES

- Abbasi, S., Rezaei, M., Keshavarzi, B., Mina, M., Ritsema, C., Geissen, V., 2021. Investigation of the 2018 Shiraz dust event: Potential sources of metals, rare earth elements, and radionuclides; health assessment. *Chemosphere* 279, 130533. <https://doi.org/10.1016/j.chemosphere.2021.130533>
- Alarcón-Aguirre, G., Sajami Quispe, E., Vásquez Zavaleta, T., Ponce Tejada, L.V., Ramos Enciso, D., Rodríguez Achata, L., Garate-Quispe, J., 2023. Vegetation dynamics in lands degraded by gold mining in the southeastern Peruvian Amazon. *Trees For. People* 11, 100369. <https://doi.org/10.1016/j.tfp.2023.100369>
- Alvares, C.A., Stape, J.L., Sentelhas, P.C., de Moraes Gonçalves, J.L., Sparovek, G., 2013. Köppen's climate classification map for Brazil. *Meteorol. Z.* 22, 711–728. <https://doi.org/10.1127/0941-2948/2013/0507>
- Araújo, S.N., Ramos, S.J., Martins, G.C., Teixeira, R.A., Souza, E.S., Sahoo, P.K., Fernandes, A.R., Gastauer, M., Caldeira, C.F., Souza-Filho, P.W.M., Dall'Agnol, R., 2021. Copper mining in the eastern Amazon: an environmental perspective on potentially toxic elements. *Environ. Geochem. Health.* <https://doi.org/10.1007/s10653-021-01051-5>
- Atibu, E.K., Lacroix, P., Sivalingam, P., Ray, N., Giuliani, G., Mulaji, C.K., Otamonga, J.-P., Mpiana, P.T., Slaveykova, V.I., Poté, J., 2018. High contamination in the areas surrounding abandoned mines and mining activities: An impact assessment of the Dilala, Luilu and Mpingiri Rivers, Democratic Republic of the Congo. *Chemosphere* 191, 1008–1020. <https://doi.org/10.1016/j.chemosphere.2017.10.052>

- Azizi, M., Faz, A., Zornoza, R., Martínez-Martínez, S., Shahrokh, V., Acosta, J.A., 2022. Environmental pollution and depth distribution of metal(loid)s and rare earth elements in mine tailing. *J. Environ. Chem. Eng.* 10, 107526. <https://doi.org/10.1016/j.jece.2022.107526>
- Banihashemi, S.R., Taheri, B., Razavian, S.M., Soltani, F., 2019. Selective Nitric Acid Leaching of Rare-Earth Elements from Calcium and Phosphate in Fluorapatite Concentrate. *JOM* 71, 4578–4587. <https://doi.org/10.1007/s11837-019-03605-6>
- Bi, X., Chu, H., Fu, M., Xu, D., Zhao, W., Zhong, Y., Wang, M., Li, K., Zhang, Y., 2023. Distribution characteristics of organic carbon (nitrogen) content, cation exchange capacity, and specific surface area in different soil particle sizes. *Sci. Rep.* 13, 12242. <https://doi.org/10.1038/s41598-023-38646-0>
- Cánovas, C.R., Macías, F., Pérez López, R., Nieto, J.M., 2018. Mobility of rare earth elements, yttrium and scandium from a phosphogypsum stack: Environmental and economic implications. *Sci. Total Environ.* 618, 847–857. <https://doi.org/10.1016/j.scitotenv.2017.08.220>
- Chen, F., Deng, Q., Wu, Yuxuan, Wu, Yuying, Chen, J., Chen, Y., Lin, L., Qiu, Y., Pan, L., Zheng, X., Wei, L., Liu, F., He, B., Wang, J., 2022. U-Shaped Relationship of Rare Earth Element Lanthanum and Oral Cancer Risk: A Propensity Score-Based Study in the Southeast of China. *Front. Public Health* 10, 905690. <https://doi.org/10.3389/fpubh.2022.905690>
- Chen, H., Chen, Zhibiao, Chen, Zhiqiang, Ou, X., Chen, J., 2020. Calculation of Toxicity Coefficient of Potential Ecological Risk Assessment of Rare Earth Elements. *Bull. Environ. Contam. Toxicol.* 104, 582–587. <https://doi.org/10.1007/s00128-020-02840-x>

Chen, H.B., Chen, H.M., Chen, Z.B., Chen, Z.Q., 2023. The ecological impacts of residues from the heap leaching of ion-adsorption rare earth clays. *Int. J. Environ. Sci. Technol.* <https://doi.org/10.1007/s13762-023-04873-1>

Chileshe, M.N., Syampungani, S., Festin, E.S., Tigabu, M., Daneshvar, A., Odén, P.C., 2020. Physico-chemical characteristics and heavy metal concentrations of copper mine wastes in Zambia: implications for pollution risk and restoration. *J. For. Res.* 31, 1283–1293. <https://doi.org/10.1007/s11676-019-00921-0>

Costis, S., Mueller, K.K., Coudert, L., Neculita, C.M., Reynier, N., Blais, J.-F., 2021. Recovery potential of rare earth elements from mining and industrial residues: A review and cases studies. *J. Geochem. Explor.* 221, 106699. <https://doi.org/10.1016/j.gexplo.2020.106699>

Covre, W.P., Ramos, S.J., Pereira, W.V. da S., Souza, E.S. de, Martins, G.C., Teixeira, O.M.M., Amarante, C.B. do, Dias, Y.N., Fernandes, A.R., 2022. Impact of copper mining wastes in the Amazon: Properties and risks to environment and human health. *J. Hazard. Mater.* 421, 126688. <https://doi.org/10.1016/j.jhazmat.2021.126688>

Cruz, R.S.D., Fernandes, C.M.D., Juliani, C., Lagler, B., Misas, C.M.E., Nascimento, T.D.S., Jesus, A.J.C.D., 2014. Química mineral do vulcano-plutonismo paleoproterozoico da região de São Félix do Xingu (PA), Cráton Amazônico. *Geol. USP Sér. Científica* 13, 97–116. <https://doi.org/10.5327/Z1519-874X201400010007>

de Lima, A.F.L., Campos, M.C.C., Martins, T.S., Silva, G.A., Brito, W.B.M., dos Santos, L.A.C., de Oliveira, I.A., da Cunha, J.M., 2022. Soil chemical attributes in areas

under conversion from forest to pasture in southern Brazilian Amazon. *Sci. Rep.* 12, 22555. <https://doi.org/10.1038/s41598-022-25406-9>

De Oliveira, C., Ramos, S.J., Siqueira, J.O., Faquin, V., De Castro, E.M., Amaral, D.C., Techio, V.H., Coelho, L.C., E Silva, P.H.P., Schnug, E., Guilherme, L.R.G., 2015. Bioaccumulation and effects of lanthanum on growth and mitotic index in soybean plants. *Ecotoxicol. Environ. Saf.* 122, 136–144. <https://doi.org/10.1016/j.ecoenv.2015.07.020>

Enang, R.K., Kips, Ph.A., Yerima, B.P.K., Kome, G.K., Van Ranst, E., 2022. Pedotransfer functions for cation exchange capacity estimation in highly weathered soils of the tropical highlands of NW Cameroon. *Geoderma Reg.* 29, e00514. <https://doi.org/10.1016/j.geodrs.2022.e00514>

Feitosa, M.M., da Silva, Y.J.A.B., Biondi, C.M., Alcantara, V.C., do Nascimento, C.W.A., 2020. Rare Earth elements in rocks and soil profiles of a tropical volcanic archipelago in the Southern Atlantic. *CATENA* 194, 104674. <https://doi.org/10.1016/j.catena.2020.104674>

Fernández-Caliani, J.C., Grantcharova, M.M., 2021. Enrichment and Fractionation of Rare Earth Elements in an Estuarine Marsh Soil Receiving Acid Discharges from Legacy Sulfide Mine Wastes. *Soil Syst.* 5, 66. <https://doi.org/10.3390/soilsystems5040066>

Ferreira, A.T.R., Lamarão, C.N., 2013. Geologia, petrografia e geoquímica das rochas vulcânicas Uatumã na Área sul de São Félix do Xingu (PA), Província Carajás. *Braz. J. Geol.* 43, 152–157. <https://doi.org/10.5327/Z2317-48892013000100013>

Ferreira, M. da S., Fontes, M.P.F., Bellato, C.R., Marques Neto, J. de O., Lima, H.N., Fendorf, S., 2021. Geochemical signatures and natural background values of rare earth elements in soils of Brazilian Amazon. Environ. Pollut. 277, 116743.  
<https://doi.org/10.1016/j.envpol.2021.116743>

Ferreira, M.D.S., Fontes, M.P.F., Pacheco, A.A., Ker, J.C., Lima, H.N., 2021. Health risks of potentially toxic trace elements in urban soils of Manaus city, Amazon, Brazil. Environ. Geochem. Health 43, 3407–3427. <https://doi.org/10.1007/s10653-021-00834-0>

Galhardi, J.A., Leles, B.P., de Mello, J.W.V., Wilkinson, K.J., 2020. Bioavailability of trace metals and rare earth elements (REE) from the tropical soils of a coal mining area. Sci. Total Environ. 717, 134484.  
<https://doi.org/10.1016/j.scitotenv.2019.134484>

Gastauer, M., Caldeira, C.F., Ramos, S.J., Trevelin, L.C., Jaffé, R., Oliveira, G., Vera, M.P.O., Pires, E., Santiago, F.L. de A., Carneiro, M.A.C., Coelho, F.T.A., Silva, R., Souza-Filho, P.W.M., Siqueira, J.-O., 2020. Integrating environmental variables by multivariate ordination enables the reliable estimation of mineland rehabilitation status. J. Environ. Manage. 256, 109894.  
<https://doi.org/10.1016/j.jenvman.2019.109894>

Gee, G.W., Bauder, J.W., 1986. Methods of Soil Analysis.

Godwyn-Paulson, P., Jonathan, M.P., Rodríguez-Espinosa, P.F., Rodríguez-Figueroa, G.M., 2022. Rare earth element enrichments in beach sediments from Santa Rosalia mining region, Mexico: An index-based environmental approach. Mar. Pollut. Bull. 174, 113271. <https://doi.org/10.1016/j.marpolbul.2021.113271>

Hakanson, L., 1980. An ecological risk index for aquatic pollution control.a sedimentological approach. Water Res. [https://doi.org/10.1016/0043-1354\(80\)90143-8](https://doi.org/10.1016/0043-1354(80)90143-8)

Hossain, M.K.; Raihan, G.A.; Akbar, M.A.; Kabir Rubel, M.H.; Ahmed, M.H.; Khan, M.I.; Hossain, S.; Sen, S.K.; Jalal, M.I.E.; El-Denglawey, A. Current Applications and Future Potential of Rare Earth Oxides in Sustainable Nuclear, Radiation, and Energy Devices: A Review. *ACS Appl. Electron. Mater.* **2022**, *4*, 3327–3353.  
<https://doi.org/10.3390/min13091186>

Jean-Lavénir, N.M., Kiki, T.N., Yiika, L.P., Ndi, G.M., 2023. Contamination, sources and risk assessments of metals in stream sediments of Pouma area, Pan-African Fold Belt, Southern Cameroon. *Water. Air. Soil Pollut.* **234**, 160.  
<https://doi.org/10.1007/s11270-023-06180-4>

Jiménez-Ballesta, R., Bravo, S., Amorós, J.Á., Pérez-de-los-Reyes, C., García-Pradas, J., Sanchez, M., García-Navarro, F.J., 2022. Occurrence of some rare earth elements in vineyard soils under semiarid Mediterranean environment. *Environ. Monit. Assess.* **194**, 341. <https://doi.org/10.1007/s10661-022-09956-z>

Jiménez-Reyes, M., Almazán-Sánchez, P.T., Solache-Ríos, M., 2021. Behaviour of cerium(III) in the presence of components of soils and its humate complex. *Environ. Technolol.* **42**, 4363–4371. <https://doi.org/10.1080/09593330.2020.1758219>

Khan, R., Islam, Md.S., Tareq, A.R.M., Naher, K., Islam, A.R.Md.T., Habib, Md.A., Siddique, Md.A.B., Islam, M.A., Das, S., Rashid, Md.B., Ullah, A.K.M.A., Miah, Md.M.H., Masrura, S.U., Bodrud-Doza, Md., Sarker, M.R., Badruzzaman, A.B.M., 2020. Distribution, sources and ecological risk of trace elements and polycyclic aromatic hydrocarbons in sediments from a polluted urban river in central

Bangladesh. Environ. Nanotechnol. Monit. Manag. 14, 100318.

<https://doi.org/10.1016/j.enmm.2020.100318>

Kotelnikova, A., Fastovets, I., Rogova, O., Volkov, D.S., Stolbova, V., 2019. Toxicity assay of lanthanum and cerium in solutions and soil. Ecotoxicol. Environ. Saf. 167, 20–28. <https://doi.org/10.1016/j.ecoenv.2018.09.117>

Kumar, V., Sharma, A., Pandita, S., Bhardwaj, R., Thukral, A.K., Cerdà, A., 2020. A review of ecological risk assessment and associated health risks with heavy metals in sediment from India. Int. J. Sediment Res. 35, 516–526. <https://doi.org/10.1016/j.ijsrc.2020.03.012>

Li, Z., Liang, T., Li, K., Wang, P., 2020. Exposure of children to light rare earth elements through ingestion of various size fractions of road dust in REEs mining areas. Sci. Total Environ. 743, 140432. <https://doi.org/10.1016/j.scitotenv.2020.140432>

Lima, M.W. de, Pereira, W.V. da S., Souza, E.S. de, Teixeira, R.A., Palheta, D. da C., Faial, K. do C.F., Costa, H.F., Fernandes, A.R., 2022. Bioaccumulation and human health risks of potentially toxic elements in fish species from the southeastern Carajás Mineral Province, Brazil. Environ. Res. 204, 112024. <https://doi.org/10.1016/j.envres.2021.112024>

Liu, H., Xu, H., Wu, Y., Ai, Z., Zhang, J., Liu, G., Xue, S., 2021. Effects of natural vegetation restoration on dissolved organic matter (DOM) biodegradability and its temperature sensitivity. Water Res. 191, 116792. <https://doi.org/10.1016/j.watres.2020.116792>

Liu, J., Dai, S., Berti, D., Eble, C.F., Dong, M., Gao, Y., Hower, J.C., 2023. Rare Earth and Critical Element Chemistry of the Volcanic Ash-fall Parting in the Fire Clay

Coal, Eastern Kentucky, USA. *Clays Clay Miner.* 71, 309–339.

<https://doi.org/10.1007/s42860-023-00237-5>

Liu, J., Wang, Z., Hu, F., Xu, C., Ma, R., Zhao, S., 2020. Soil organic matter and silt contents determine soil particle surface electrochemical properties across a long-term natural restoration grassland. *CATENA* 190, 104526.

<https://doi.org/10.1016/j.catena.2020.104526>

Liu, Q., Shi, H., An, Y., Ma, J., Zhao, W., Qu, Y., Chen, H., Liu, L., Wu, F., 2023. Source, environmental behavior and potential health risk of rare earth elements in Beijing urban park soils. *J. Hazard. Mater.* 445, 130451.

<https://doi.org/10.1016/j.jhazmat.2022.130451>

Lu, X., Zhang, X., Li, L.Y., Chen, H., 2014. Assessment of metals pollution and health risk in dust from nursery schools in Xi'an, China. *Environ. Res.* 128, 27–34.

<https://doi.org/10.1016/j.envres.2013.11.007>

Mabagala, F.S., Mng'ong'o, M.E., 2022. On the tropical soils; The influence of organic matter (OM) on phosphate bioavailability. *Saudi J. Biol. Sci.* 29, 3635–3641.

<https://doi.org/10.1016/j.sjbs.2022.02.056>

Medas, D., Cidu, R., De Giudici, G., Podda, F., 2013. Geochemistry of rare earth elements in water and solid materials at abandoned mines in SW Sardinia (Italy). *J. Geochem. Explor.* 133, 149–159. <https://doi.org/10.1016/j.gexplo.2013.05.005>

Mihajlovic, J., Bauriegel, A., Stärk, H.-J., Roßkopf, N., Zeitz, J., Milbert, G., Rinklebe, J., 2019. Rare earth elements in soil profiles of various ecosystems across Germany. *Appl. Geochem.* 102, 197–217. <https://doi.org/10.1016/j.apgeochem.2019.02.002>

- Mîndrescu, M., Haliuc, A., Zhang, W., Carozza, L., Carozza, J.-M., Groparu, T., Valette, P., Sun, Q., Nian, X., Gradinaru, I., 2022. A 600 years sediment record of heavy metal pollution history in the Danube Delta. *Sci. Total Environ.* 823, 153702. <https://doi.org/10.1016/j.scitotenv.2022.153702>
- Mor, S., Vig, N., Ravindra, K., 2022. Distribution of heavy metals in surface soil near a coal power production unit: potential risk to ecology and human health. *Environ. Monit. Assess.* 194, 263. <https://doi.org/10.1007/s10661-021-09692-w>
- Moreira, L.J.D., da Silva, E.B., Fontes, M.P.F., Liu, X., Ma, L.Q., 2018. Speciation, bioaccessibility and potential risk of chromium in Amazon forest soils. *Environ. Pollut.* 239, 384–391. <https://doi.org/10.1016/j.envpol.2018.04.025>
- Nwaila, G.T., Ghorbani, Y., Zhang, S.E., Frimmel, H.E., Tolmay, L.C.K., Rose, D.H., Nwaila, P.C., Bourdeau, J.E., 2021. Valorisation of mine waste - Part I: Characteristics of, and sampling methodology for, consolidated mineralised tailings by using Witwatersrand gold mines (South Africa) as an example. *J. Environ. Manage.* 295, 113013. <https://doi.org/10.1016/j.jenvman.2021.113013>
- Ou, X., Chen, Zhibiao, Chen, X., Li, X., Wang, J., Ren, T., Chen, H., Feng, L., Wang, Y., Chen, Zhiqiang, Liang, M., Gao, P., 2022. Redistribution and chemical speciation of rare earth elements in an ion–adsorption rare earth tailing, Southern China. *Sci. Total Environ.* 821, 153369. <https://doi.org/10.1016/j.scitotenv.2022.153369>
- Padoan, E., Romè, C., Mehta, N., Dino, G.A., De Luca, D.A., Ajmone-Marsan, F., 2021. Bioaccessibility of metals in soils surrounding two dismissed mining sites in Northern Italy. *Int. J. Environ. Sci. Technol.* 18, 1349–1360. <https://doi.org/10.1007/s13762-020-02938-z>

Pereira, W.V. da S., Ramos, S.J., Melo, L.C.A., Braz, A.M. de S., Dias, Y.N., Almeida, G.V. de, Fernandes, A.R., 2022. Levels and environmental risks of rare earth elements in a gold mining area in the Amazon. Environ. Res. 211, 113090.  
<https://doi.org/10.1016/j.envres.2022.113090>

Pereira, W.V. da S., Ramos, S.J., Melo, L.C.A., Dias, Y.N., Martins, G.C., Ferreira, L.C.G., Fernandes, A.R., 2023. Human and environmental exposure to rare earth elements in gold mining areas in the northeastern Amazon. Chemosphere 340, 139824. <https://doi.org/10.1016/j.chemosphere.2023.139824>

Pereira, W.V. da S., Teixeira, R.A., Souza, E.S. de, Moraes, A.L.F. de, Campos, W.E.O., Amarante, C.B. do, Martins, G.C., Fernandes, A.R., 2020. Chemical fractionation and bioaccessibility of potentially toxic elements in area of artisanal gold mining in the Amazon. J. Environ. Manage. 267, 110644.  
<https://doi.org/10.1016/j.jenvman.2020.110644>

Pyrgaki, K., Gemeni, V., Karkalis, C., Koukouzas, N., Koutsovitis, P., Petrounias, P., 2021. Geochemical Occurrence of Rare Earth Elements in Mining Waste and Mine Water: A Review. Minerals 11, 860. <https://doi.org/10.3390/min11080860>

Quesada, C.A., Paz, C., Oblitas Mendoza, E., Phillips, O.L., Saiz, G., Lloyd, J., 2020. Variations in soil chemical and physical properties explain basin-wide Amazon forest soil carbon concentrations. SOIL 6, 53–88. <https://doi.org/10.5194/soil-6-53-2020>

R Core Team, 2023. R: A language and environment for statistical computing.

Ramos, F.T., Dores, E.F.G. de C., Weber, O.L. dos S., Beber, D.C., Campelo, J.H., Maia, J.C. de S., 2018. Soil organic matter doubles the cation exchange capacity of

tropical soil under no-till farming in Brazil. *J. Sci. Food Agric.* 98, 3595–3602.

<https://doi.org/10.1002/jsfa.8881>

Rudnick, R.L., Fountain, D.M., 1995. Nature and composition of the continental crust: A lower crustal perspective. *Rev. Geophys.* 33, 267.

<https://doi.org/10.1029/95RG01302>

Saha, B., Eliason, K., Golui, D., Masud, J., Bezbaruah, A.N., Iskander, S.M., 2023. Rare earth elements in sands collected from Southern California sea beaches. *Chemosphere* 344, 140254. <https://doi.org/10.1016/j.chemosphere.2023.140254>

Saleh, H.M., Eskander, S.B., Mahmoud, H.H., Abdelaal, S.A., 2022. Study on rare earth elements, heavy metals and organic contents in the soil of oil exploration site at Matruh Governorate, Egypt. *Results Geophys. Sci.* 9, 100039.

<https://doi.org/10.1016/j.ringps.2021.100039>

Sergeeva, A., Zinicovscaia, I., Grozdov, D., Yushin, N., 2021. Assessment of selected rare earth elements, HF, Th, and U in the Donetsk region using moss bags technique. *Atmospheric Pollut. Res.* 12, 101165.

<https://doi.org/10.1016/j.apr.2021.101165>

Silva, F.B.V., Nascimento, C.W.A., Alvarez, A.M., Araújo, P.R.M., 2019. Inputs of rare earth elements in Brazilian agricultural soils via P-containing fertilizers and soil correctives. *J. Environ. Manage.* 232, 90–96.

<https://doi.org/10.1016/j.jenvman.2018.11.031>

Silva, Fernanda Rodrigues da., Barros, M. A. S. A., Pierosan, R., Pinho, F. E. C., Rocha, M. L. B. P., Vasconcelos, B. R., Dezula, S. E. M., Tavares, C., Rocha, J. Geoquímica e geocronologia UCPb (SHRIMP) de granitos da região de Peixoto

de Azeiedo: Proíncia Aurífera Alta Floresta, Mato Grosso. Brazilian Journal of Geology, São Paulo, i. 44, n. 3, p. 433C455, jul./set. 2014.  
<http://dx.doi.org/10.5327/22317C4889201400030007>.

Sojka, M., Choiński, A., Ptak, M., Siepak, M., 2021. Causes of variations of trace and rare earth elements concentration in lakes bottom sediments in the Bory Tucholskie National Park, Poland. Sci. Rep. 11, 244. <https://doi.org/10.1038/s41598-020-80137-z>

Soltani, F., Abdollahy, M., Petersen, J., Ram, R., Javad Koleini, S.M., Moradkhani, D., 2019. Leaching and recovery of phosphate and rare earth elements from an iron-rich fluorapatite concentrate: Part II: Selective leaching of calcium and phosphate and acid baking of the residue. Hydrometallurgy 184, 29–38. <https://doi.org/10.1016/j.hydromet.2018.12.024>

Souza, E.S. de, Fernandes, A.R., De Souza Braz, A.M., Oliveira, F.J. de, Alleoni, L.R.F., Campos, M.C.C., 2018. Physical, chemical, and mineralogical attributes of a representative group of soils from the eastern Amazon region in Brazil. SOIL 4, 195–212. <https://doi.org/10.5194/soil-4-195-2018>

Souza Neto, H.F. de, Pereira, W.V. da S., Dias, Y.N., Souza, E.S. de, Teixeira, R.A., Lima, M.W. de, Ramos, S.J., Amarante, C.B. do, Fernandes, A.R., 2020. Environmental and human health risks of arsenic in gold mining areas in the eastern Amazon. Environ. Pollut. 265, 114969. <https://doi.org/10.1016/j.envpol.2020.114969>

Su, H., Zhang, D., Antwi, P., Xiao, L., Deng, X., Liu, Z., Long, B., Shi, M., Manefield, M.J., Ngo, H.H., 2021. Exploring potential impact(s) of cerium in mining

wastewater on the performance of partial-nitrification process and nitrogen conversion microflora. *Ecotoxicol. Environ. Saf.* 209, 111796.  
<https://doi.org/10.1016/j.ecoenv.2020.111796>

Sun, G., Li, Z., Liu, T., Chen, J., Wu, T., Feng, X., 2017. Rare earth elements in street dust and associated health risk in a municipal industrial base of central China. *Environ. Geochem. Health* 39, 1469–1486. <https://doi.org/10.1007/s10653-017-9982-x>

Sutherland, R.A., 2000. Bed sediment-associated trace metals in an urban stream, Oahu, Hawaii. *Environ. Geol.* 39, 611–627.

Teixeira, P.C., Donagemma, G.K., Fontana, A., Teixeira, W.G., 2017. Manual de métodos de análise de solo, 3. ed. rev. ed. Embrapa, Brasília, DF.

Teixeira, R.A., Pereira, W.V. da S., Souza, E.S. de, Ramos, S.J., Dias, Y.N., Lima, M.W. de, de Souza Neto, H.F., Oliveira, E.S. de, Fernandes, A.R., 2021. Artisanal gold mining in the eastern Amazon: Environmental and human health risks of mercury from different mining methods. *Chemosphere* 284, 131220.  
<https://doi.org/10.1016/j.chemosphere.2021.131220>

Thomas, P.J., Carpenter, D., Boutin, C., Allison, J.E., 2014. Rare earth elements (REEs): Effects on germination and growth of selected crop and native plant species. *Chemosphere* 96, 57–66. <https://doi.org/10.1016/j.chemosphere.2013.07.020>

Tomlinson, D.L., Wilson, J.G., Harris, C.R., Jeffrey, D.W., 1980. Problems in the assessment of heavy-metal levels in estuaries and the formation of a pollution index. *Helgoländer Meeresunters.* 33, 566–575. <https://doi.org/10.1007/BF02414780>

USEPA, 2001. Supplemental guidance for developing soil screening levels for superfund sites. Office of Solid Waste and Emergency Response, Washington.

Velásquez Ramírez, M.G., Barrantes, J.A.G., Thomas, E., Gamarra Miranda, L.A., Pillaca, M., Tello Peramas, L.D., Bazán Tapia, L.R., 2020. Heavy metals in alluvial gold mine spoils in the peruvian amazon. *CATENA* 189, 104454.  
<https://doi.org/10.1016/j.catena.2020.104454>

Venegas, V.H.A., Novais, R.F., Barros, N.F., Cantarutti, R.B., LOPES, A.S., 1999. Interpretation of soil analysis results, in: Recommendations for the Use of Correctives and Fertilizers in Minas Gerais. Comissão de Fertilidade do Solo do Estado de Minas Gerais, Viçosa, pp. 25–32.

Wang, X.M., Hu, J.Z., Peng, C., Wen, W.J., Ou, H., 2021. Distribution and Potential Ecological Risk Assessment of Four Light Rare Earth Elements in the Anning River Located in Sichuan Province, China. *IOP Conf. Ser. Earth Environ. Sci.* 849, 012001. <https://doi.org/10.1088/1755-1315/849/1/012001>

Wang, Y., Wang, G., Sun, M., Liang, X., He, H., Zhu, J., Takahashi, Y., 2022. Environmental risk assessment of the potential “Chemical Time Bomb” of ion-adsorption type rare earth elements in urban areas. *Sci. Total Environ.* 822, 153305.  
<https://doi.org/10.1016/j.scitotenv.2022.153305>

Wu, J., Lu, J., Li, L., Min, X., Zhang, Z., Luo, Y., 2019a. Distribution, pollution, and ecological risks of rare earth elements in soil of the northeastern Qinghai–Tibet Plateau. *Hum. Ecol. Risk Assess. Int. J.* 25, 1816–1831.  
<https://doi.org/10.1080/10807039.2018.1475215>

Wu, J., Lu, J., Li, L., Min, X., Zhang, Z., Luo, Y., 2019b. Distribution, pollution, and ecological risks of rare earth elements in soil of the northeastern Qinghai–Tibet Plateau. *Hum. Ecol. Risk Assess. Int. J.* 25, 1816–1831.  
<https://doi.org/10.1080/10807039.2018.1475215>

Zerizghi, T., Guo, Q., Wei, R., Wang, Z., Du, C., Deng, Y., 2023. Rare earth elements in soil around coal mining and utilization: Contamination, characteristics, and effect of soil physicochemical properties. *Environ. Pollut.* 331, 121788.  
<https://doi.org/10.1016/j.envpol.2023.121788>

## SUPPLEMENTARY MATERIAL

**Table 1S.**

Location of sampling points.

Areas	Sample	Latitude (S)	Longitude (W)
OV1	S1	06°04'08.4"S	52°11'20.4"W
	S2	06°04'8.04"S	52°11'27.6"W
	S3	06°04'19.2"S	52°11'30.2"W
	S4	06°04'37.2"S	52°11'31.0"W
	S5	06°04'40.8"S	52°11'31.2"W
	S6	06°04'48"S	52°11'31.8"W
	S7	06°04'26.4"S	52°11'38.4"W
	S8	06°04'48"S	52°11'38.1"W
	S9	06°04'58.8"S	52°11'42"W
	S10	06°04'16.8"S	52°11'49"W
TA1	S1	06°04'12"S	52°11'24"W
	S2	06°04'15.6"S	52°11'27.6"W
	S3	06°04'22.8"S	52°11'27.6"W
	S4	06°04'30"S	52°11'31.2"W
	S5	06°04'44.4"S	52°11'31.2"W
	S6	06°04'37.2"S	52°11'34.8"W
	S7	06°04'9.6"S	52°11'38.4"W
	S8	06°04'2404"S	52°11'49.2"W
OV2	S1	06°01'55.2"S	52°14'27.6"S
	S2	06°01'58.8"S	52°14'31.2"S
	S3	06°02'9.6"S	52°14'25.6"S

	S4	06°02'24"S	52°14'31.2"S
TA2	S1	06°02'2.4"S	52°14'27.6"S
	S2	06°02'20.4"S	52°14'31.2"S
	S3	06°02'27.6"S	52°14'27.6"S
OV3	S1	06°03'46.8"S	52°11'06"S
	S2	06° 03'43.2"S	52°10'58.8"S
	S3	06° 03'50.4"S	52°11'9.6"S
	S4	06° 03'28.8"S	52°10'55.2"S
TA3	S1	06° 03'18"S	52°10'51.6"S
	S2	06° 03'36"S	52°10'50.2"S
	S3	06° 03'33"S	52°10'48"S
RA	S1	06°04'30"S	52°09'57.6"S
	S2	06°04'15.6"S	52°09'37.4"S
	S3	06°04'44.4"S	52°09'37.6"S

**Table 2S.**

Recovery rate of REEs in analytical batches.

Element	Reference material	Certified value	Obtained value	Recovery rate (%)
Ce	OREAS 142	180.5	156.9	86.9
Dy	OREAS 142	5.25	4.8	91.4
Er	OREAS 142	2.91	2.7	92.8
Eu	OREAS 142	2.22	1.4	63.1
Gd	OREAS 142	7.56	6.4	84.6
Ho	OREAS 142	1.01	0.9	89.1
La	OREAS 142	92.5	78.7	85.1
Lu	OREAS 142	0.36	0.27	75.0
Nd	OREAS 142	66.4	48.6	73.2
Pr	OREAS 142	19.35	15.8	81.6
Sc	OREAS 142	65.71	43.2	65.7
Sm	OREAS 142	9.8	8.2	83.6
Tb	OREAS 142	1.05	1.0	95.2
Tm	OREAS 142	0.39	0.3	76.9
Y	OREAS 142	29.21	23.9	81.8
Yb	OREAS 142	2.7	2.5	92.6

**Table 3S.**

Cargas fatoriais obtidas em análise de componentes principais entre propriedades de amostras e concentrações de REEs.

Properties	Dimension 1	Dimension 2
Clay	0.819806	0.22781
Sand	-0.82926	-0.50073
Silt	0.419418	0.642902
CEC	0.730082	-0.09232
OC	0.69191	0.143597
$\sum$ LREE	-0.63683	0.700689
$\sum$ HREE	-0.68941	0.663423

**Table 4S.**

Potential ecological risk factors (PERF) of REEs in the studied areas.

Element	Areas					
	OV1	TA1	OV2	TA2	OV3	TA3
Ce	2.0	3.5	10.9	15.5	1.9	0.8
Dy	11.0	11.0	24.5	53.5	9.5	2.5
Er	10.0	10.5	16.5	41.5	12.5	2.5
Eu	22.0	26.0	43.0	105.0	3.0	29.0
Gd	12.5	18.0	44.0	77.0	7.5	3.5
Ho	21.0	22.0	38.0	90.0	21.0	5.0
La	2.2	4.3	14.1	19.8	3.5	0.8
Lu	32.0	30.0	46.0	114.0	70.0	8.0
Nd	4.6	9.0	27.6	38.6	3.8	1.4
Pr	10.5	21.0	64.5	92.5	12.0	3.0
Sc	4.3	7.7	4.5	43.4	6.8	7.0
Sm	12.5	20.5	60.0	89.0	8.5	3.5
Tb	25.0	31.0	65.0	129.0	19.0	6.0
Tm	19.0	18.0	29.0	72.0	29.0	5.0
Y	4.6	4.8	7.8	19.8	4.8	1.2
Yb	9.0	8.0	8.0	31.0	19.0	2.0

**Table 5S.**

Health risk quotients for adults due to exposure to REEs.

Element	Non-carcinogenic						Carcinogenic					
	OV1	TA1	OV2	TA2	OV3	TA3	OV1	TA1	OV2	TA2	OV3	TA3
Ce	$2.3 \times 10^{-3}$	$1.3 \times 10^{-2}$	$2.4 \times 10^{-2}$	$2.8 \times 10^{-2}$	$2.6 \times 10^{-3}$	$3.8 \times 10^{-3}$	$7.7 \times 10^{-17}$	$4.4 \times 10^{-16}$	$7.9 \times 10^{-16}$	$9.4 \times 10^{-16}$	$8.5 \times 10^{-17}$	$1.3 \times 10^{-16}$
Dy	$1.7 \times 10^{-4}$	$6.1 \times 10^{-4}$	$7.0 \times 10^{-4}$	$1.3 \times 10^{-3}$	$1.3 \times 10^{-4}$	$1.7 \times 10^{-4}$	$5.7 \times 10^{-18}$	$2.0 \times 10^{-17}$	$2.3 \times 10^{-17}$	$4.3 \times 10^{-17}$	$4.5 \times 10^{-18}$	$5.7 \times 10^{-18}$
Er	$1.4 \times 10^{-4}$	$4.4 \times 10^{-4}$	$4.3 \times 10^{-4}$	$8.9 \times 10^{-4}$	$1.1 \times 10^{-4}$	$1.4 \times 10^{-4}$	$4.7 \times 10^{-18}$	$1.5 \times 10^{-17}$	$1.4 \times 10^{-17}$	$3.0 \times 10^{-17}$	$3.6 \times 10^{-18}$	$4.6 \times 10^{-18}$
Eu	$5.0 \times 10^{-6}$	$2.0 \times 10^{-5}$	$1.8 \times 10^{-5}$	$2.6 \times 10^{-5}$	$7.6 \times 10^{-6}$	$2.7 \times 10^{-5}$	$1.7 \times 10^{-19}$	$6.5 \times 10^{-19}$	$6.0 \times 10^{-19}$	$8.6 \times 10^{-19}$	$2.5 \times 10^{-19}$	$8.9 \times 10^{-19}$
Gd	$1.2 \times 10^{-4}$	$5.5 \times 10^{-4}$	$8.1 \times 10^{-4}$	$1.2 \times 10^{-3}$	$1.1 \times 10^{-4}$	$1.4 \times 10^{-4}$	$4.1 \times 10^{-18}$	$1.8 \times 10^{-17}$	$2.7 \times 10^{-17}$	$3.9 \times 10^{-17}$	$3.6 \times 10^{-18}$	$4.8 \times 10^{-18}$
Ho	$4.0 \times 10^{-5}$	$1.3 \times 10^{-4}$	$1.4 \times 10^{-4}$	$2.7 \times 10^{-4}$	$3.1 \times 10^{-5}$	$3.9 \times 10^{-5}$	$1.3 \times 10^{-18}$	$4.4 \times 10^{-18}$	$4.6 \times 10^{-18}$	$9.1 \times 10^{-18}$	$1.0 \times 10^{-18}$	$1.3 \times 10^{-18}$
La	$1.1 \times 10^{-3}$	$6.5 \times 10^{-3}$	$1.3 \times 10^{-2}$	$1.5 \times 10^{-2}$	$1.2 \times 10^{-3}$	$1.6 \times 10^{-3}$	$3.5 \times 10^{-17}$	$2.2 \times 10^{-16}$	$4.2 \times 10^{-16}$	$4.9 \times 10^{-16}$	$4.1 \times 10^{-17}$	$5.3 \times 10^{-17}$
Lu	$2.9 \times 10^{-5}$	$7.9 \times 10^{-5}$	$7.5 \times 10^{-5}$	$1.6 \times 10^{-4}$	$2.3 \times 10^{-5}$	$2.8 \times 10^{-5}$	$9.8 \times 10^{-19}$	$2.6 \times 10^{-18}$	$2.5 \times 10^{-18}$	$5.3 \times 10^{-18}$	$7.6 \times 10^{-19}$	$9.5 \times 10^{-19}$
Nd	$6.8 \times 10^{-4}$	$4.1 \times 10^{-3}$	$7.6 \times 10^{-3}$	$8.9 \times 10^{-3}$	$7.4 \times 10^{-4}$	$8.7 \times 10^{-4}$	$2.3 \times 10^{-17}$	$1.4 \times 10^{-16}$	$2.5 \times 10^{-16}$	$3.0 \times 10^{-16}$	$2.4 \times 10^{-17}$	$2.9 \times 10^{-17}$
Pr	$2.1 \times 10^{-4}$	$1.3 \times 10^{-3}$	$2.4 \times 10^{-3}$	$2.9 \times 10^{-3}$	$2.4 \times 10^{-4}$	$2.7 \times 10^{-4}$	$7.1 \times 10^{-18}$	$4.3 \times 10^{-17}$	$8.0 \times 10^{-17}$	$9.6 \times 10^{-17}$	$8.0 \times 10^{-18}$	$8.8 \times 10^{-18}$
Sc	$6.6 \times 10^{-5}$	$4.4 \times 10^{-4}$	$1.3 \times 10^{-4}$	$1.5 \times 10^{-4}$	$1.2 \times 10^{-4}$	$4.4 \times 10^{-4}$	$2.2 \times 10^{-18}$	$1.5 \times 10^{-17}$	$4.3 \times 10^{-18}$	$5.0 \times 10^{-18}$	$4.0 \times 10^{-18}$	$1.5 \times 10^{-17}$
Sm	$1.3 \times 10^{-4}$	$6.8 \times 10^{-4}$	$1.2 \times 10^{-3}$	$1.5 \times 10^{-3}$	$1.3 \times 10^{-4}$	$1.5 \times 10^{-4}$	$4.4 \times 10^{-18}$	$2.3 \times 10^{-17}$	$4.0 \times 10^{-17}$	$5.0 \times 10^{-17}$	$4.4 \times 10^{-18}$	$5.1 \times 10^{-18}$
Tb	$2.5 \times 10^{-5}$	$9.4 \times 10^{-5}$	$1.2 \times 10^{-4}$	$2.0 \times 10^{-4}$	$2.1 \times 10^{-5}$	$2.6 \times 10^{-5}$	$8.3 \times 10^{-19}$	$3.1 \times 10^{-18}$	$4.0 \times 10^{-18}$	$6.7 \times 10^{-18}$	$6.9 \times 10^{-19}$	$8.7 \times 10^{-19}$
Tm	$2.4 \times 10^{-5}$	$7.0 \times 10^{-5}$	$6.8 \times 10^{-5}$	$1.4 \times 10^{-4}$	$1.9 \times 10^{-5}$	$2.4 \times 10^{-5}$	$8.1 \times 10^{-19}$	$2.3 \times 10^{-18}$	$2.3 \times 10^{-18}$	$4.6 \times 10^{-18}$	$6.2 \times 10^{-19}$	$7.9 \times 10^{-19}$
Y	$1.3 \times 10^{-3}$	$3.9 \times 10^{-3}$	$4.0 \times 10^{-3}$	$8.4 \times 10^{-3}$	$9.5 \times 10^{-4}$	$1.2 \times 10^{-3}$	$4.2 \times 10^{-17}$	$1.3 \times 10^{-16}$	$1.3 \times 10^{-16}$	$2.8 \times 10^{-16}$	$3.2 \times 10^{-17}$	$4.1 \times 10^{-17}$
Yb	$1.9 \times 10^{-4}$	$5.1 \times 10^{-4}$	$4.9 \times 10^{-4}$	$1.0 \times 10^{-3}$	$1.5 \times 10^{-4}$	$1.8 \times 10^{-4}$	$6.4 \times 10^{-18}$	$1.7 \times 10^{-17}$	$1.6 \times 10^{-17}$	$3.5 \times 10^{-17}$	$5.0 \times 10^{-18}$	$6.1 \times 10^{-18}$

**Table 6S.**

Health risk quotients for children due to exposure to REEs.

Element	Non-carcinogenic						Carcinogenic					
	OV1	TA1	OV2	TA2	OV3	TA3	OV1	TA1	OV2	TA2	OV3	TA3
Ce	$2.0 \times 10^{-2}$	$1.1 \times 10^{-1}$	$2.1 \times 10^{-1}$	$2.5 \times 10^{-1}$	$2.2 \times 10^{-2}$	$3.3 \times 10^{-2}$	$6.8 \times 10^{-16}$	$3.8 \times 10^{-15}$	$6.9 \times 10^{-15}$	$8.2 \times 10^{-15}$	$7.5 \times 10^{-16}$	$1.1 \times 10^{-15}$
Dy	$1.5 \times 10^{-3}$	$5.3 \times 10^{-3}$	$6.1 \times 10^{-3}$	$1.1 \times 10^{-2}$	$1.2 \times 10^{-3}$	$1.5 \times 10^{-3}$	$5.0 \times 10^{-17}$	$1.8 \times 10^{-16}$	$2.0 \times 10^{-16}$	$3.7 \times 10^{-16}$	$3.9 \times 10^{-17}$	$5.0 \times 10^{-17}$
Er	$1.2 \times 10^{-3}$	$3.8 \times 10^{-3}$	$3.7 \times 10^{-3}$	$7.8 \times 10^{-3}$	$9.6 \times 10^{-4}$	$1.2 \times 10^{-3}$	$4.1 \times 10^{-17}$	$1.3 \times 10^{-16}$	$1.2 \times 10^{-16}$	$2.6 \times 10^{-16}$	$3.2 \times 10^{-17}$	$4.0 \times 10^{-17}$
Eu	$4.3 \times 10^{-5}$	$1.7 \times 10^{-4}$	$1.6 \times 10^{-4}$	$2.3 \times 10^{-4}$	$6.7 \times 10^{-5}$	$2.3 \times 10^{-4}$	$1.4 \times 10^{-18}$	$5.7 \times 10^{-18}$	$5.3 \times 10^{-18}$	$7.5 \times 10^{-18}$	$2.2 \times 10^{-18}$	$7.8 \times 10^{-18}$
Gd	$1.1 \times 10^{-3}$	$4.8 \times 10^{-3}$	$7.1 \times 10^{-3}$	$1.0 \times 10^{-2}$	$9.4 \times 10^{-4}$	$1.3 \times 10^{-3}$	$3.6 \times 10^{-17}$	$1.6 \times 10^{-16}$	$2.4 \times 10^{-16}$	$3.4 \times 10^{-16}$	$3.1 \times 10^{-17}$	$4.2 \times 10^{-17}$
Ho	$3.5 \times 10^{-4}$	$1.1 \times 10^{-3}$	$1.2 \times 10^{-3}$	$2.4 \times 10^{-3}$	$2.7 \times 10^{-4}$	$3.4 \times 10^{-4}$	$1.2 \times 10^{-17}$	$3.8 \times 10^{-17}$	$4.0 \times 10^{-17}$	$7.9 \times 10^{-17}$	$9.1 \times 10^{-18}$	$1.1 \times 10^{-17}$
La	$9.2 \times 10^{-3}$	$5.7 \times 10^{-2}$	$1.1 \times 10^{-1}$	$1.3 \times 10^{-1}$	$1.1 \times 10^{-2}$	$1.4 \times 10^{-2}$	$3.1 \times 10^{-16}$	$1.9 \times 10^{-15}$	$3.7 \times 10^{-15}$	$4.3 \times 10^{-15}$	$3.6 \times 10^{-16}$	$4.7 \times 10^{-16}$
Lu	$2.6 \times 10^{-4}$	$6.9 \times 10^{-4}$	$6.6 \times 10^{-4}$	$1.4 \times 10^{-3}$	$2.0 \times 10^{-4}$	$2.5 \times 10^{-4}$	$8.6 \times 10^{-18}$	$2.3 \times 10^{-17}$	$2.2 \times 10^{-17}$	$4.6 \times 10^{-17}$	$6.6 \times 10^{-18}$	$8.3 \times 10^{-18}$
Nd	$5.9 \times 10^{-3}$	$3.6 \times 10^{-2}$	$6.6 \times 10^{-2}$	$7.8 \times 10^{-2}$	$6.4 \times 10^{-3}$	$7.6 \times 10^{-3}$	$2.0 \times 10^{-16}$	$1.2 \times 10^{-15}$	$2.2 \times 10^{-15}$	$2.6 \times 10^{-15}$	$2.1 \times 10^{-16}$	$2.5 \times 10^{-16}$
Pr	$1.9 \times 10^{-3}$	$1.1 \times 10^{-2}$	$2.1 \times 10^{-2}$	$2.5 \times 10^{-2}$	$2.1 \times 10^{-3}$	$2.3 \times 10^{-3}$	$6.2 \times 10^{-17}$	$3.8 \times 10^{-16}$	$7.0 \times 10^{-16}$	$8.4 \times 10^{-16}$	$7.0 \times 10^{-17}$	$7.7 \times 10^{-17}$
Sc	$5.8 \times 10^{-4}$	$3.9 \times 10^{-3}$	$1.1 \times 10^{-3}$	$1.3 \times 10^{-3}$	$1.1 \times 10^{-3}$	$3.8 \times 10^{-3}$	$1.9 \times 10^{-17}$	$1.3 \times 10^{-16}$	$3.8 \times 10^{-17}$	$4.4 \times 10^{-17}$	$3.5 \times 10^{-17}$	$1.3 \times 10^{-16}$
Sm	$1.2 \times 10^{-3}$	$5.9 \times 10^{-3}$	$1.1 \times 10^{-2}$	$1.3 \times 10^{-2}$	$1.1 \times 10^{-3}$	$1.3 \times 10^{-3}$	$3.9 \times 10^{-17}$	$2.0 \times 10^{-16}$	$3.5 \times 10^{-16}$	$4.3 \times 10^{-16}$	$3.8 \times 10^{-17}$	$4.5 \times 10^{-17}$
Tb	$2.2 \times 10^{-4}$	$8.2 \times 10^{-4}$	$1.1 \times 10^{-3}$	$1.8 \times 10^{-3}$	$1.8 \times 10^{-4}$	$2.3 \times 10^{-4}$	$7.3 \times 10^{-18}$	$2.7 \times 10^{-17}$	$3.5 \times 10^{-17}$	$5.8 \times 10^{-17}$	$6.0 \times 10^{-18}$	$7.6 \times 10^{-18}$
Tm	$2.1 \times 10^{-4}$	$6.1 \times 10^{-4}$	$6.0 \times 10^{-4}$	$1.2 \times 10^{-3}$	$1.6 \times 10^{-4}$	$2.1 \times 10^{-4}$	$7.1 \times 10^{-18}$	$2.0 \times 10^{-17}$	$2.0 \times 10^{-17}$	$4.0 \times 10^{-17}$	$5.4 \times 10^{-18}$	$6.9 \times 10^{-18}$
Y	$1.1 \times 10^{-2}$	$3.4 \times 10^{-2}$	$3.5 \times 10^{-2}$	$7.4 \times 10^{-2}$	$8.3 \times 10^{-3}$	$1.1 \times 10^{-2}$	$3.7 \times 10^{-16}$	$1.1 \times 10^{-15}$	$1.2 \times 10^{-15}$	$2.5 \times 10^{-15}$	$2.8 \times 10^{-16}$	$3.6 \times 10^{-16}$
Yb	$1.7 \times 10^{-3}$	$4.5 \times 10^{-3}$	$4.3 \times 10^{-3}$	$9.1 \times 10^{-3}$	$1.3 \times 10^{-3}$	$1.6 \times 10^{-3}$	$5.6 \times 10^{-17}$	$1.5 \times 10^{-16}$	$1.4 \times 10^{-16}$	$3.0 \times 10^{-16}$	$4.4 \times 10^{-17}$	$5.3 \times 10^{-17}$

## CAPÍTULO 2

### Metais pesados em mineração artesanal na Amazônia: concentração e risco potencial da exploração de cassiterita e monazita

#### Resumo

A extração de minerais, como a cassiterita, é imprescindível para fornecer matéria prima para diversas tecnologias. Entretanto, os processos artesanais de exploração liberam vários elementos, como os elementos potencialmente tóxicos (EPTs), representando risco potencial ao ambiente e a saúde humana. O objetivo foi quantificar as concentrações de EPTs e estimar a contaminação e poluição ambiental em áreas de mineração artesanal de cassiterita na região amazônica. Os materiais estudados foram classificados como resíduos de mineração artesanal, sendo garimpo ativo (TA1) (8 amostras), garimpo desativado a um ano TA2 (3 amostras) e garimpo desativado a dez anos (TA3) (3 amostras) além de área de referência (3 amostras). As concentrações totais de As, Ba, Cd, Cr, Mo, Ni e Pb foram extraídas por digestão ácida (HCl: HNO<sub>3</sub> 3:1) em forno microondas. Os resultados das concentrações foram utilizados para calcular fator de bioacumulação e índices de poluição, risco ambiental e a saúde humana. Pb (TA3) e Cr (TA1 e 3) apresentaram concentrações acima do valor de prevenção do CONAMA, o que indicando risco potencial. O fator de contaminação indicou alta contaminação ainda que a área explorada estivesse sem utilização a 10 anos, indicando alta capacidade de acumulação. A bioacumulação foi considerável ( $>1$ ) para todos os EPTs relacionando diretamente com as características químicas dos resíduos, como: pouca matéria orgânica, baixa soma de bases e pH ácido, favorecendo a absorção de metais pelas plantas.

#### Palavras chave:

Elementos terras raras, Mineração artesanal, Risco ambiental, Contaminação, Poluição.

## **Abstract**

The extraction of minerals, such as cassiterite, is essential for providing raw materials for various technologies. However, artisanal mining processes release several elements, including potentially toxic elements (PTEs), posing potential risks to the environment and human health. The objective was to quantify PTE concentrations and estimate environmental contamination and pollution in areas of artisanal cassiterite mining in the Amazon region. The materials studied were classified as artisanal mining residues, including an active mining site (TA1) (8 samples), a site deactivated for one year (TA2) (3 samples), and a site deactivated for ten years (TA3) (3 samples), as well as a reference area (3 samples). Total concentrations of As, Ba, Cd, Cr, Mo, Ni, and Pb were extracted through acid digestion (HCl: HNO<sub>3</sub> 3:1) in a microwave oven. The concentration results were used to calculate the bioaccumulation factor, pollution indices, and environmental and human health risks. Pb (TA3) and Cr (TA1 and TA3) showed concentrations above the prevention threshold set by CONAMA, indicating potential risk. The contamination factor indicated high contamination, even in areas that had been unused for 10 years, demonstrating a high capacity for accumulation. Bioaccumulation was considerable (>1) for all PTEs, directly related to the chemical characteristics of the residues, such as low organic matter, low base saturation, and acidic pH, which favor metal absorption by plants.

## **Keywords**

Amazônia, Mineração artesanal, Risco ambiental, Contaminação, Poluição.

## **1. INTRODUÇÃO**

A mineração industrial, é uma atividade importante para a geração de economia e postos de trabalho (Matlaba, et al 2019), em sua maioria atende critérios estabelecidos por entidades de proteção aos interesses ambientais e sociais, de modo a representar menor risco. Porém, na região amazônica as atividades de exploração artesanal são realidade e representam grande parte dos garimpos espalhados na região, e a geração de resíduos desse sistema, podem causar danos significativos ao ecossistema local e à saúde, especialmente devido à falta informações a respeito dos riscos provenientes da exploração desses minerais (Pereira et al, 2022; Neto et al,2020; Covre et al, 2022).

As atividades de mineração artesanal têm sido responsáveis por grande parcela da extração mineral do país, principalmente na região norte, que em função da sua grande extensão territorial, tem os processos de fiscalização prejudicados. A cassiterita é um mineral rico em elementos terras raras (família dos lantanídeos, além do escândio e do ítrio). Para obtenção desses elementos, é necessário realizar o desmonte mecânico da área a ser explorada, causando instabilidade provocada pelos processos físico-químicos, podendo também representar riscos ao ambiente e a saúde (Souza et al, 2019; Neto et al, 2020; Covre et al, 2022). Esse processo de exploração, ocorre de forma desordenada, sem seguir os critérios e legislação impostas para essa atividade, o que causa a mobilização de diversos elementos, entre eles os EPTs, que podem representar risco ambiental e a saúde humana.

Os (PTEs) originam-se de fontes litogênicas via pedogênese e ocorrendo em baixas concentrações de forma natural. A ocorrência de níveis além do normal pode ser resultado de atividades humanas, como: atividades industriais, emissão de poluentes urbanos, agricultura e atividades de mineração ou de origem natural em áreas com alto potencial

de depósito mineral (Reimann et al. 2016). Assim, quantificar a concentração e os riscos potenciais desses elementos se tornam necessários para evitar catástrofes e a contaminação para a população (Lima et al, 2020).

A utilização de índices que estimem esses riscos, se torna necessários para prever, mitigar e recuperar os efeitos nocivos de elementos contaminantes (Abbasi et al., 2021; Jean-Lavenir et al., 2023; Sojka et al., 2021). Deste modo, o objetivo foi determinar as concentrações de EPTs em áreas artesanalmente já exploradas e em exploração para obtenção cassiterita e monazita e quantificar os níveis de risco ambientais nessas áreas.

## **2. MATERIAL E MÉTODOS**

### **Área de estudo e amostragem**

A área de estudo está inserida em São Félix do Xingu ( $06^{\circ}37'48''$  S e  $51^{\circ}57'36''$  W) município localizado no sudeste do estado do Pará. É a segunda maior cidade brasileira, conta com  $84.213\text{ km}^2$  de extensão e aproximadamente 136.000 habitantes (IBGE, 2022). O clima predominante na região é o tropical úmido, classificado como Am de acordo com a classificação de Koppen, com temperatura média anual de  $26^{\circ}\text{C}$  (Alvares et al., 2013).

Há predominância nas formações geológicas Sobreiro e Santa Rosa, não metamorfoseadas e sob pouca transformação intempérica (Silva et al., 2014; Cruz et al., 2014). Na região, áreas de mineração artesanal de cassiterita e monazita ocupam grandes extensões.

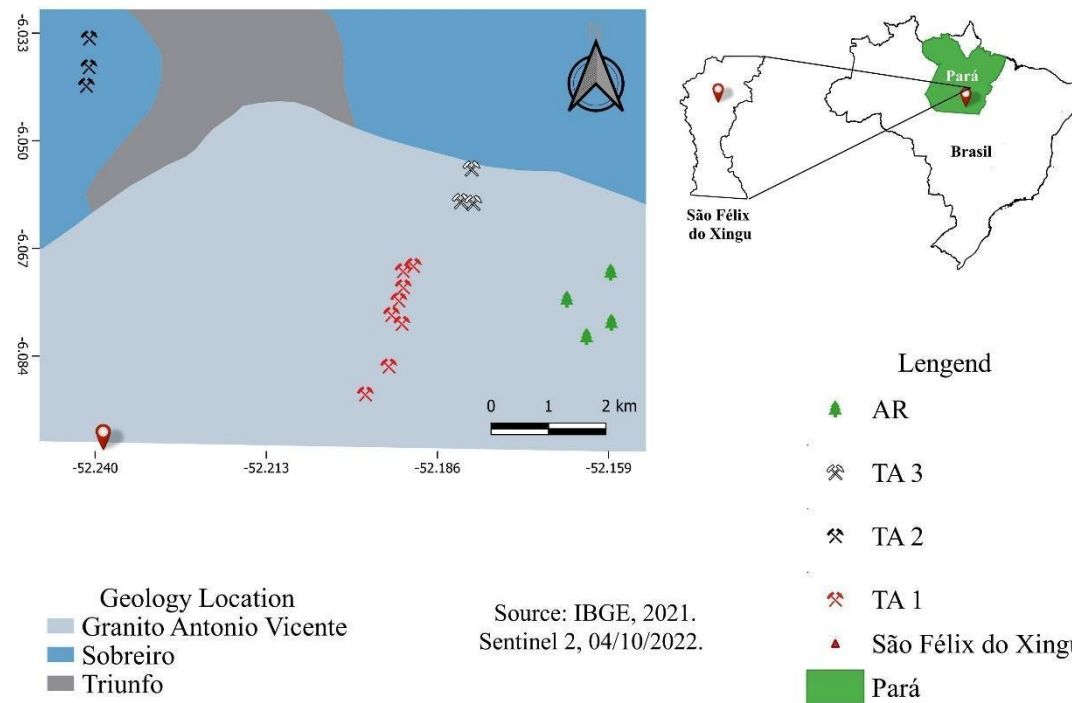
A extração de Cassiterita na região é realizada irregularmente, com exploração a céu aberto com desmonte mecânico, através do uso de máquinário, gerando o material indicado como estéril, após é realizado o desmonte hidráulico, gerando material

semelhante a lama que será processado. Porém, em função da falta de padronização dos métodos de obtenção do minério e de descarte dos resíduos, fica impossibilitada a segregação do material descartado, sendo assim classificado como resíduo.

As áreas foram identificadas como: TA1 = rejeitos de mina ativa (8 amostras); TA2 = rejeitos de minas desativadas há um ano (3 amostras); TA3 = rejeitos de minas desativadas há 10 anos (3 amostras); e RA= solo de floresta natural (4 amostras), considerada como referência (Figura 1).

**Figura 1.**

Pontos de amostragem de resíduos de mineração artesanal de monazita e cassiterita no município de São Félix do Xingu, sudeste da Amazônia brasileira.



As amostras de plantas foram coletadas nos mesmos pontos de coleta do solo onde existia vegetação, objetivando estimar a capacidade de bioacumulação de EPT's. A coleta de *Brachiaria brizantha*, foi realizada com o corte a altura do solo.

## **Caracterização de amostras de solo, planta e fator de bioacumulação**

Os atributos físico-químicos foram realizados conforme método proposto por Teixeira et al. (2017). As amostras foram homogeneizadas e secas ao ar, depois peneiradas (< 2 mm) e armazenadas em recipientes de polietileno. O pH foi determinado em suspensão de solo: água: (1:2,5) e solução de KCl 1 mol L<sup>-1</sup>. Os cátions trocáveis Ca<sup>2+</sup>, Mg<sup>2+</sup> e Al<sup>3+</sup> foram extraídos usando KCl 1 mol L<sup>-1</sup>. O Al<sup>3+</sup> foi quantificado por titulação com NaOH 0,025 M e Ca<sup>2+</sup> e Mg<sup>2+</sup> foram quantificados por complexometria com EDTA 0,0125 mol L<sup>-1</sup>. K e P disponíveis foram extraídos usando solução Mehlich-1 (0,05 mol L<sup>-1</sup> HCl + 0,0125 mol L<sup>-1</sup> H<sub>2</sub>SO<sub>4</sub>).

Carbono orgânico foi determinado por combustão úmida com dicromato de potássio e multiplicado por 1,72 para determinar o teor de matéria orgânica (OM). A acidez potencial (H<sup>+</sup> + Al<sup>3+</sup>) foi determinada com acetato de cálcio (Ca(C<sub>2</sub>H<sub>3</sub>O<sub>2</sub>)<sub>2</sub>) tamponado em pH 7,0. Os resultados foram utilizados para calcular a capacidade de troca catiônica (CEC). A textura do solo foi determinada pelo método da pipeta (Gee and Bauder, 1986).

Para concentrações totais de PTE foram utilizados 0,5 g de amostras de solo (< 0,15 mm) com 9 mL de HNO<sub>3</sub> e 3 mL de HCl concentrado, digeridos em forno de micro-ondas conforme EPA 3051A (USEPA, 2007). Os extratos digeridos foram diluídos em água deionizada até um volume final de 50 mL e filtrados (0,45 µm PTFE). Ba, Cd, Co, Cu, Cr, Mo, Ni e Pb e quantificadas por espectrometria de massa com plasma indutivamente acoplado (ICP-MS, PerkinElmer).

Os teores de EPTs do tecido vegetal foram extraídos por digestão ácida por micro-ondas, utilizando a adição de 2 mL de HNO<sub>3</sub> + 2 mL de H<sub>2</sub>O<sub>2</sub> e 5 mL de água ultrapura a 250 mg de amostra (Araújo et al., 2002), e quantificadas por espectrometria de massa com plasma indutivamente acoplado (ICP-MS, PerkinElmer).

O fator de bioacumulação (BAF) tem sido amplamente utilizado para entender o grau de acumulação de um determinado contaminante no tecido vegetal (Covre et al., 2020), encontrado de acordo com a Equação:

$$BAF = (C_p / C_s)$$

onde  $C_p$  é a concentração de EPT no tecido vegetal (peso seco) e  $C_s$  é a concentração do mesmo EPT no solo.

### Avaliação da poluição

Foram calculados o fator de contaminação (CF), fator de enriquecimento (EF) e do índice de carga poluente (PLI), a fim de estimar o nível de contaminação (Khan et al., 2020; Sergeeva et al., 2021; Zerizghi et al., 2023). Para os cálculos, RA foi considerada como referência de ambiente natural, devido ao baixo impacto das atividades de mineração nessa área, conforme sugerido por estudos anteriores (Araújo et al., 2021; Covre et al., 2020; Pereira et al., 2022; Souza Neto et al., 2020).

O CF é um índice para avaliar o nível de poluição associado ao EPT em áreas antropizadas (Godwyn-Paulson et al., 2022; Jiménez-Ballesta et al., 2022; Wang et al., 2022), obtido de acordo com a Eq. (1):

$$CF = \frac{C_{EPT}}{B_{EPT}} \quad (1)$$

onde  $C_{EPT}$  é a concentração média do EPT ( $\text{mg kg}^{-1}$ ) na área alterada e  $B_{EPT}$  é a concentração do mesmo EPT em RA. Os valores de CF foram interpretados da seguinte forma:  $CF < 1$  indica contaminação baixa,  $CF$  entre  $1 - 3$  indica contaminação moderada,  $CF$  entre  $3 - 6$  indica contaminação considerável, e  $CF > 6$  indica contaminação alta (Hakanson, 1980).

O EF foi calculado para identificar o nível de enriquecimento associado aos EPTs (Azizi et al., 2022; Saleh et al., 2022; Zerizghi et al., 2023), conforme a Eq. (2):

$$EF = \left( \frac{C_{EPT}}{C_{Fe}} / \frac{B_{EPT}}{B_{Fe}} \right) \quad (2)$$

onde  $C_{EPT}$  é a concentração do EPT na amostra,  $C_{Fe}$  é a concentração de Fe na mesma amostra ( $\text{mg kg}^{-1}$ ),  $B_{EPT}$  é a concentração do EPT em RA, e  $B_{Fe}$  é a concentração de Fe em RA. O Fe foi usado para normalização geoquímica devido ao seu comportamento conservador (Pereira et al., 2022). Os valores de EF foram interpretados da seguinte forma: EF < 2 indica enriquecimento mínimo, EF entre 2 – 5 indica enriquecimento moderado, EF entre 5 – 20 indica enriquecimento significativo, EF entre 20 – 40 indica enriquecimento alto, e EF > 40 indica enriquecimento extremo (Sutherland, 2000).

O PLI é utilizado para estimar a poluição cumulativa de determinado grupo de elementos (Abbasi et al., 2021; Jean-Lavenir et al., 2023; Sojka et al., 2021), obtido conforme a Eq. (3):

$$PLI = (CF_1 \times CF_2 \times CF_3 \times \dots \times CF_n)^{1/n} \quad (3)$$

onde CF é o fator de contaminação e n é o número de EPTs do estudo. Os valores de PLI foram classificados em dois níveis: PLI variando de 0 a 1 indica ausência de poluição e PLI > 1 indica material poluído (Tomlinson et al., 1980).

### **Avaliação de risco ambiental**

O fator de risco ecológico potencial (PERF) e o índice de risco ecológico potencial (PERI) foram calculados para avaliar os impactos dos EPTs para o ecossistema nas áreas estudadas (Q. Liu et al., 2023; Pereira et al., 2023; Saha et al., 2023). O PERF permite conhecer os riscos ecológicos individuais dos elementos em áreas alteradas pela

mineração. Nesse estudo, o EF foi incorporado ao cálculo do PERF (Kumar et al., 2020; Lima et al., 2022), de acordo com a Eq. (4):

$$PERF_{EPT} = EF_{EPT} \times TRF_{EPT} \quad (4)$$

Onde CF<sub>PTE</sub> é o fator de contaminação do PTE, TR é o fator de resposta tóxica do respectivo PTE (As = 10, Ba = Cr = 2, Cd = 30, Cu = Ni = Pb = 5, Mo = 1) (Hakanson, 1980; Shangguan et al., 2015; Yang et al., 2015; Ngole-Jeme and Fantke, 2017). Os resultados foram interpretados da seguinte forma: PERF < 40 indica baixo risco, PERF entre 40 – 80 indica risco moderado, PERF entre 80 – 160 indica risco considerável, PERF entre 160 – 320 indica risco alto, e PERF > 320 indica risco muito alto (Hakanson, 1980).

O PERI permite conhecer os efeitos da ação conjunta dos EPTs no ecossistema (Chen et al., 2020; Wang et al., 2021; Wu et al., 2019b), encontrado de acordo com a Eq. (5):

$$PERI = PERF_1 + PERF_2 + PERF_3 + \dots + PERF_n \quad (5)$$

onde PERF é o fator de risco ecológico potencial e n é o número de elementos em estudo. Os valores de PERI foram interpretados da seguinte forma: PERI < 150 indica baixo risco, PERI entre 150 – 300 indica risco moderado, PERI entre 300 – 600 indica risco considerável, e PERI > 600 indica risco muito alto (Hakanson, 1980).

## Análises estatísticas

Os resultados foram submetidos à análise estatística descritiva e de normalidade dos dados (Shapiro-Wilk). A comparação entre as áreas foi avaliada com o teste de Kruskal-Wallis e o teste Dunn. A análise de componentes principais (PCA) foi gerada para compreender o relacionamento entre as concentrações de EPTs e as propriedades

físico-químicas dos materiais. Todas as análises foram realizadas usando o software R versão 4.3.1 (R Core Team, 2023).

## RESULTADOS E DISCUSSÃO

### Caracterização dos resíduos de mineração e concentração de EPTs

Nas áreas de mineração artesanal (TA1, TA2 e TA3), foram encontradas concentrações de cromo (Cr) e chumbo (Pb) superiores aos valores de prevenção (CONAMA, 2009). No solo da área de referência, nenhum dos EPTs observados no estudo foram superiores aos valores de prevenção (Fernandes et al, 2018). As atividades de extração de cassiterita e monazita, que envolvem a desagregação das rochas, podem resultar na liberação significativa desses contaminantes no solo. As atividades realizadas durante a mineração artesanal propiciam a elevação dos teores de EPTs, devido a alocação de materiais nas áreas próximas aos locais de exploração mineral (Souza et al., 2017).

Os valores de pH das amostras variaram entre 4,5 e 4,9 (tabela 1S), caracterizando um ambiente ácido em todas as áreas avaliadas. Ambientes tropicais comumente tem solos com características ácidas devido à elevada precipitação que proporciona a lixiviação de bases trocáveis e a ciclagem de material orgânico, durante esse processo ocorre a acidificação do meio (Awoonor *et al.*, 2024). O uso excessivo de água, observado durante o processo de exploração artesanal, pode auxiliar na lixiviação de compostos básicos, facilitando a acidificação do meio e influenciando na mobilidade de EPTs, os quais se tornam mais solúveis em condições de baixa alcalinidade, proporcionando o aumento da bioacumulação/ transporte de contaminantes para o ambiente (Huang et al., 2020).

A matéria orgânica (MO) nos solos variou de 20,0 g dm<sup>-3</sup> em TA1 a 57,7 g dm<sup>-3</sup> na área de referência (tabela 1S). Os maiores níveis de MO em áreas nativas (florestas)

são característicos de ambientes com diversidade florestal, já em áreas de exploração mineral comumente ocorre uma elevada perda de MO devido a supressão que ocorre durante a exploração mineral. A MO desempenha um papel essencial na dinâmica da bioacumulação de EPTs, sendo reconhecida por sua capacidade de retenção de EPTs, assim limitando a disponibilidade para a absorção pelas plantas. Os EPTs formam complexos com a MO, o que reduz a mobilidade e a toxicidade desses elementos, comumente os ácidos húmicos e fúlvicos, são eficazes na ligação com cátions metálicos, dificultando a absorção das formas solúveis de EPTs pelas raízes das plantas e contribuindo para a imobilização desses contaminantes no solo (García et al., 2021; Pereira et al., 2022). Nos materiais avaliados, a MO foi baixa, os elementos ficam disponíveis para serem absorvidos pelas plantas ou serem translocados para outros ambientes, o que justifica a alta concentração desses contaminantes nos resíduos.

A capacidade de troca de cátions (CTC) nas amostras de solo varia significativamente, influenciando a retenção de contaminantes. A área TA2, com uma CTC de apenas  $1,1 \text{ cmolc dm}^{-3}$ , apresenta a menor capacidade de retenção de nutrientes, o que pode facilitar a lixiviação de EPTs.

A heterogeneidade química das concentrações de EPTs nos solos de floresta e nos resíduos de mineração de cassiterita e monazita é evidente (Tabela 2). Tal diversidade pode ser atribuída à formação mineralógica heterogênea e à falta de padronização nos processos de extração artesanal, que variam em profundidade, quantidade de material utilizado e maquinário, resultando em diversidade na composição desses resíduos (Chileshe et al., 2020; Perlatti et al., 2015; Souza Neto et al., 2020).

Os processos mecânicos (escavação e Trituração) e exposição dessas rochas/minerais durante a exploração mineral, junto ao descarte inadequado de rejeitos, favorecem a liberação de EPTs e a mobilização desses elementos, provocando a

contaminação do solo, ar, água e plantas (Diame et al., 2016). Esse cenário representa um risco significativo à saúde da população local, portanto, torna-se imprescindível quantificar essas concentrações e estudar os níveis de contaminação e os riscos ambientais associados à saúde humana.

**Tabela 2.**

Concentração de EPTs nas áreas estudadas.

Elemento ( $\text{mg kg}^{-1}$ )	TA1	TA2	TA3	RA	PV	QRV
As	$3.3 \pm 1.8$ a	$1.0 \pm 0.0$ c	$1.6 \pm 0.5$ b	$1.8 \pm 0.9$ b	15	1.4
Ba	$19.1 \pm 1.1$ b	$12.0 \pm 1.9$ c	$79.0 \pm 16.5$ a	$6.9 \pm 0.1$ d	150	14.3
Cd	$0.0 \pm 0.0$ b	$0.7 \pm 1.3$ a	$0.0 \pm 0.0$ b	$0.9 \pm 0.0$ a	1.3	0.4
Cr	$93.2 \pm 11.0$ b	$25.6 \pm 4.2$ c	$170.3 \pm 17.0$ a	$15.5 \pm 0.6$ d	75	24.1
Cu	$47.9 \pm 4.6$ a	$12.0 \pm 7.7$ c	$20.1 \pm 5.2$ b	$5.7 \pm 0.0$ d	60	9.9
Mo	$3.2 \pm 0.5$ a	$2.6 \pm 0.7$ a	$2.7 \pm 0.6$ a	$1.0 \pm 0.0$ b	30	0.1
Ni	$8.1 \pm 1.7$ b	$2.3 \pm 0.8$ c	$21.0 \pm 3.5$ a	$1.4 \pm 0.2$ c	30	1.4
Al	19400	2900	54433	2.9	-	-
Fe	42500	20830	28266	33.0	-	-
Mn	772.5	942	1657	72	-	-
Pb	$35.6 \pm 4.4$ c	$49.2 \pm 7.5$ b	$74.7 \pm 5.0$ a	$8.4 \pm 1.4$ d	72	4.8

\*letras diferentes na horizontal representam diferença significativa

**Tabela 3.**

Fator de contaminação (FC), fator de enriquecimento (EF) e índice de risco ecológico potencial (PERI) de EPTs.

Element	TA1		TA2		TA3	
	CF	EF	CF	EF	CF	EF
As	1.8 ± 1.4	0.4 ± 0.3	0.5 ± 0.0	0.3 ± 0.2	3.3 ± 1.9	0.4 ± 0.2
Ba	2.7 ± 0.7	0.7 ± 0.3	1.7 ± 0.1	0.8 ± 0.3	11.4 ± 1.4	1.4 ± 0.3
Cd	0.0 ± 0.0	0.0 ± 0.0	0.8 ± 0.3	0.7 ± 1.3	0.0 ± 0.0	0.0 ± 0.3
Cr	6.0 ± 1.2	1.1 ± 0.5	1.7 ± 0.9	0.8 ± 0.3	10.9 ± 1.7	1.2 ± 0.3
Cu	8.3 ± 1.7	1.5 ± 0.8	2.1 ± 0.8	0.8 ± 0.0	3.5 ± 0.9	0.7 ± 0.0
Mo	3.0 ± 1.3	0.7 ± 0.4	2.4 ± 0.5	0.8 ± 0.1	2.5 ± 1.4	0.8 ± 0.1
Ni	5.6 ± 0.9	1.1 ± 0.4	1.6 ± 0.6	0.9 ± 0.4	14.4 ± 1.0	1.6 ± 0.4
Pb	4.3 ± 0.5	1.3 ± 0.8	5.9 ± 1.4	13.4 ± 1.1	8.8 ± 1.5	24.6 ± 1.1
PERI	49.5		57.1		77.4	
PLI	0.8		0.7		1.9	

EF < 2 indica enriquecimento mínimo, EF entre 2 – 5 indica enriquecimento moderado, EF entre 5 – 20 indica enriquecimento significativo, EF entre 20 – 40 indica enriquecimento alto, e EF > 40 indica enriquecimento extremo

CF < 1 indica contaminação baixa, CF entre 1 – 3 indica contaminação moderada, CF entre 3 – 6 indica contaminação considerável, e CF > 6 indica contaminação alta

**Tabela 4.**Teor médio de EPTs em plantas, solo ( $\text{mg kg}^{-1}$ ) e fator de bioacumulação (BAF).

Elemento	Planta			BAF		
	TA1	TA2	TA3	TA1	TA2	TA3
As	1,0 ± 0,3 b	1,3 ± 0,1 b	2,7 ± 0,3 a	3,3	0,8	0,6
Ba	61,0 ± 5,2 a	66,7 ± 1,2 a	48,7 ± 2,2 b	0,3	0,2	1,6
Cd	0,1 ± 0,1 a	0,1 ± 0,1 a	0,1 ± 0,1 a	0,0	5,8	0,0
Cr	11,7 ± 2,1 c	34,3 ± 6,2 b	95,0 ± 5,3 a	8,0	0,7	1,8
Cu	17,9 ± 3,1 c	31,7 ± 2,7 b	67,2 ± 7,0 a	2,7	0,4	0,3
Mo	1,6 ± 0,5 b	2,3 ± 0,9 b	19,2 ± 2,1 a	2,0	0,9	0,1
Ni	5,9 ± 0,9 c	10,9 ± 3,2 b	35,8 ± 4,1 a	1,4	0,2	0,6
Pb	4,0 ± 0,6 c	10,1 ± 1,1 a	7,7 ± 1,9 b	9,0	4,9	9,7

A área de estudo apresenta concentrações de Cr e Pb acima dos valores de qualidade e prevenção estabelecidos, as atividades de mineração artesanal podem ter aumentado as concentrações desses elementos em área superficial em relação ao ambiente natural (área de referência), o que foi evidenciado através do fator de contaminação (FC), com resultados variados entre os diferentes materiais estudados (Tabela 3). As áreas de exploração artesanal apresentam enriquecimento alto para Pb em TA2 e TA3 com FE 13.4 e 24.6, respectivamente. Em TA1 a contaminação variou de moderada a alta, 1.8 (As) e 8.3 (Cu) a exceção do Cd. TA2 apresentou contaminação moderada para Ba, Cr, Cu, Mo, Ni e contaminação considerável para Pb. TA3 apresentou as maiores contaminações, variando de moderada 2.5 (Mo) à alta para Pb (8.8), Cr (10.9), Ba (11.4) e Ni (14.4) (Tabela 3).

O FC indica alta contaminação por EPTs e o FE indicou que apenas o Pb, apresentou enriquecimento, mesmo após 10 anos do processo de exploração artesanal de cassiterita e monazita, o que indica alta capacidade de acumulação e pouco transporte desses EPTs nos resíduos gerados. Nessas áreas, pode ocorrer a movimentação de partículas pelo vento e pela água, o que pode ter causado a dispersão de partículas ricas em EPTs contribuindo para o enriquecimento de Pb nessas áreas (Anaman et al., 2022).

Além dos maiores teores de Fe/Al/Mn nessa área, os quais minimizam perdas por lixiviação devido a retenção propiciadas pelos minerais ricos nesses elementos.

Os índices de risco ecológico potencial revelaram que a contaminação e o enriquecimento de EPTs nas áreas mineradas do Taboca, variando de baixo a moderado. Risco ecológico em decorrência da mineração também foi encontrado em solos de Hunan, na China, com contribuição direta das altas concentrações de Pb e Zn em áreas próximas aos pontos de exploração mineral (Lu et al., 2015).

As concentrações dos PTEs variaram entre as diferentes amostras de plantas de *B. brizantha* coletadas nas áreas de mineração em São Félix do Xingu (Tabela 4). A amostragem de plantas foi realizada em áreas onde há descarte e consequente amontoa de resíduos da extração, local onde foi realizada as amostragens do resíduo estudado. A absorção e bioacumulação de PTE's nas plantas dependem da disponibilidade destes no solo, que por sua vez depende das propriedades do solo, como pH, argila, óxidos, teores de MO e CTC (Chen et al., 2014; Zhuang et al., 2014). Os solos das áreas de amostragem de plantas apresentaram baixas concentrações de MO e baixa soma de bases e baixo pH, o que favorece a absorção de metais pelas plantas.

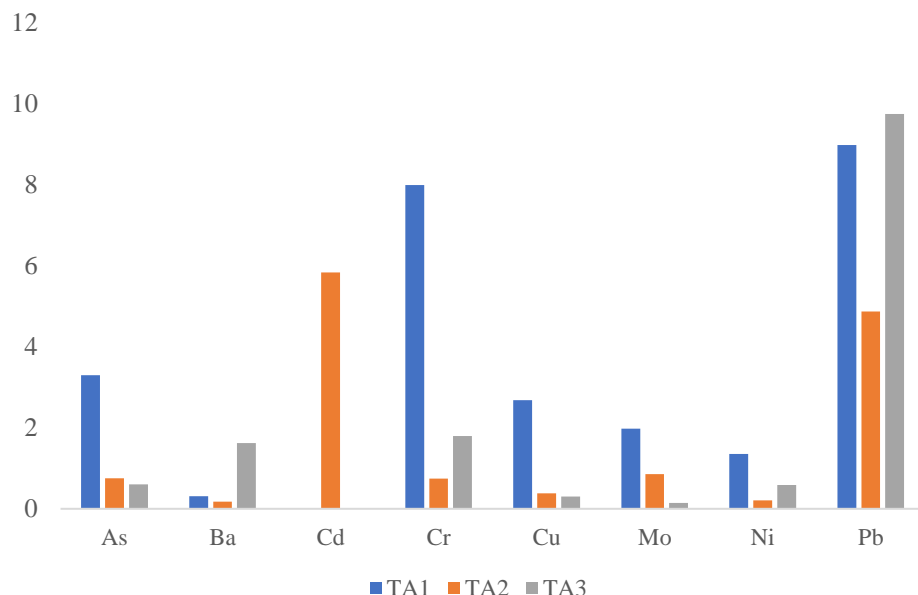


**Figura 2.**

Fator de bioacumulação de EPTs em áreas de mineração artesanal de monazita e cassiterita, ativas e desativadas a um e dez anos, no distrito da Taboca, São Félix do Xingu, estado do Pará.

As concentrações médias de EPTs nos tecidos vegetais variaram, em TA1 0,1 mg kg<sup>-1</sup> (As) a 61,0 mg kg<sup>-1</sup> (Ba), em TA2 0,1 mg kg<sup>-1</sup> (Cd) a 66,7 mg kg<sup>-1</sup> (Ba), e TA3

0,1 mg kg<sup>-1</sup> (Cd) e 95,7 mg kg<sup>-1</sup> (Cr). Os fatores de bioacumulação variaram em TA1 0,3 Ba e 9,0 para Pb, em TA2 0,2 (Ba e Ni) e 5,8 (Cd), TA3 ocorreu variação de 0,1 (Mo) e 9,7 (Pb) (Figura 2; Tabela 4). Esses valores de bioacumulação, revelam que *B. Brizantha* representa risco de bioacumulação de EPTs o que pode representar risco de acumulação na cadeia alimentar, o que é potencial risco à saúde da população que reside na região como aos consumidores do rebanho bovino que se alimenta dessa forrageira. O Pb, elemento que quando causa contaminação em áreas agrícolas, eleva o risco de bioacumulação em seres humanos (Costa et al., 2020; Bamagoos et al., 2022).

BAF elevado para cádmio em TA2, onde o pH é baixo (4,6), destaca como a acidez do solo pode facilitar a absorção desses contaminantes pelas plantas, aumentando assim os riscos à saúde dos consumidores finais na cadeia alimentar. Os dados corroboram com estudos onde plantas forrageiras de *Urochloa brizantha* submetidas a solos contaminados com Pb demonstram bioacumulação considerável, sendo possível a sua utilização como fitorremediadora (Farnezi et al. 2023), porém na região de São Félix do Xingu, onde se tem o maior rebanho bovino do estado do Pará com aproximadamente 2,5 milhões de cabeças de gado (IBGE, 2023) o risco de bioacumulação através do consumo dessa carne pode representar alto risco para a população.

A análise de componentes principais permitiu explicar 57% da variabilidade total dos dados (PC 1= 39% e PC2= 18%) (Fig. 2).

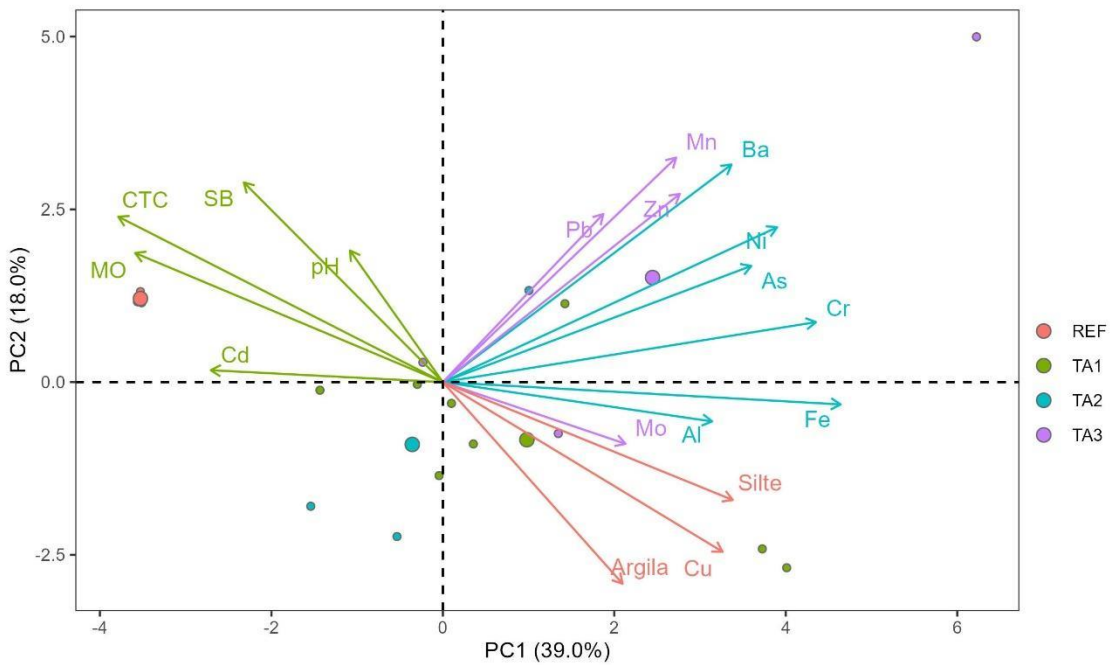


**Figura 3.**

Análise de componentes principais (PCA) entre propriedades amostrais e concentrações de EPTs nas áreas estudadas.

A PC1 é representada (loadings>0,5) negativamente (Cd, pH, CTC, SB e MO) e positivamente (Fe, Al, As, Ba, Cr, Cu, Mn, Ni, Zn e Silte). A PC2 é representada (loadings>0,5) negativamente (Argila) e positivamente (Ba, Mn, Zn e SB). Cargas elevadas e forte relação foram observados para CTC (0,75), MO (0,71), o que pode ser explicado pela maior atividade química da MO, que geram cargas negativas para a retenção de cátions (Bi *et al.*, 2023; Liu *et al.*, 2020). Além disso, forte relacionamento foi evidenciado entre Ba, Ni, As, Cr, Fe e Al, o que reforça o comportamento e a origem semelhantes desses elementos.

## **CONCLUSÃO**

É evidente a contaminação por EPTs nas áreas de mineração artesanal de monazita e cassiterita. As altas concentrações de cromo (Cr) e chumbo (Pb), superam os limites de segurança estabelecidos e sugerem risco potencial para a biota e para a saúde humana, evidenciados pelo fator de contaminação, fator de enriquecimento, risco ecológico potencial e pela bioacumulação em plantas, destacando a urgência de ações integradas que abordam tanto os impactos ambientais da mineração quanto a saúde pública, especialmente em uma região com uma população significativa de bovinos. Os dados reforçam a necessidade urgente de estratégias de mitigação, como práticas de reabilitação de áreas mineradas e monitoramento contínuo das concentrações de EPTs. A implementação de medidas para minimizar a exposição dos seres humanos e da fauna aos contaminantes é crucial, dado o papel das plantas forrageiras na cadeia alimentar da região.

## REFERENCIAS

- Abbasi, S., Rezaei, M., Keshavarzi, B., Mina, M., Ritsema, C., Geissen, V., 2021. Investigation of the 2018 Shiraz dust event: Potential sources of metals, rare earth elements, and radionuclides; health assessment. *Chemosphere* 279, 130533.  
<https://doi.org/10.1016/j.chemosphere.2021.130533>
- GCL Araújo, MH Gonzalez, AG Ferreira, ARA, Nogueira, JA, Nóbrega. (2002). Efeito da concentração de ácido na digestão assistida por micro-ondas em recipiente fechado de materiais vegetais. *Spectrochim. Acta Parte B At. Spectrosc.*, 57 (2002) , pp. 2121 - 2132 , [10.1016/S0584-8547\(02\)00164-7](https://doi.org/10.1016/S0584-8547(02)00164-7)
- Alvares, C.A., Stape, J.L., Sentelhas, P.C., De Moraes Gonçalves, J.L., Sparovek, G., 2013. Köppen's climate classification map for Brazil. *Meteorol. Z.* 22, 711–728.  
<https://doi.org/10.1127/0941-2948/2013/0507>
- Araújo, S.N., Ramos, S.J., Martins, G.C., Teixeira, R.A., Souza, E.S., Sahoo, P.K., Fernandes, A.R., Gastauer, M., Caldeira, C.F., Souza-Filho, P.W.M., Dall'agnol, R., 2021. Copper mining in the eastern Amazon: an environmental perspective on potentially toxic elements. *Environ. Geochem. Health.*  
<https://doi.org/10.1007/s10653-021-01051-5>
- Awoonor, J.K; Amoako, E.E; Dogbey, B.F; Wiredu, I. Quantitative analysis of soil degradation in response to land use change in the Guinea savanna zone of Ghana, *Geoderma Regional*, Volume 37, 2024, e00779, ISSN 2352-0094.  
<https://doi.org/10.1016/j.geodrs.2024.e00779>
- Azizi, M., Faz, A., Zornoza, R., Martínez-Martínez, S., Shahrokh, V., Acosta, J.A., 2022. Environmental pollution and depth distribution of metal(loid)s and rare earth elements in mine tailing. *J. Environ. Chem. Eng.* 10, 107526.  
<https://doi.org/10.1016/j.jece.2022.107526>

BAMAGOOS, A. A. et al. Alleviating lead-induced phytotoxicity and enhancing the phytoremediation of castor bean (*Ricinus communis* L.) by glutathione application: new insights into the mechanisms regulating antioxidants, gas exchange and lead uptake. International Journal of Phytoremediation, v. 24, n. 9, p. 933-944, 2022. DOI: 10.1080/15226514.2021.1985959.

COSTA, L. V. D. et al. Teor de chumbo nos alimentos da região nordeste do Brasil: uma revisão integrativa. Brazilian Journal of Health Review, v. 3, n. 3, p. 6823-6842, 2020. DOI: 10.34119/bjhrv3n3-220

Covre, W.P., Ramos, S.J., Pereira, W.V. Da S., Souza, E.S. De, Martins, G.C., Teixeira, O.M.M., Amarante, C.B. Do, Dias, Y.N., Fernandes, A.R., 2022. Impact of copper mining wastes in the Amazon: Properties and risks to environment and human health. J. Hazard. Mater. 421, 126688.

<https://doi.org/10.1016/j.jhazmat.2021.126688>

Cruz, R.S.D., Fernandes, C.M.D., Juliani, C., Lagler, B., Misas, C.M.E., Nascimento, T.D.S., Jesus, A.J.C.D., 2014. Química mineral do vulcão-plutônio paleoproterozoico da região de São Félix do Xingu (PA), Cráton Amazônico. Geol. USP Sér. Científica 13, 97–116. <https://doi.org/10.5327/Z1519-874X201400010007>

De Souza, E. S.; Dias, Y. N.; Da Costa, H. S. C.; Pinto, D. A.; De Oliveira, D.; De S. F., N.; Teixeira, R. A.; Fernandes, A. R. Organic residues and biochar to immobilize potentially toxic elements in soil from a gold mine in the Amazon. Ecotoxicology and environmental safety, v. 169, p. 425-434, 2019.

Diami, S.M., Kusin, F.M. & Madzin, Z. Potential ecological and human health risks of heavy metals in surface soils associated with iron ore mining in Pahang, Malaysia.

Environ Sci Pollut Res 23, 21086–21097 (2016). <https://doi.org/10.1007/s11356-016-7314-9>

Farnezi, MMdM; Silva, EdB; Santos, LLD; Silva, AC; Grazziotti, PH; Alleoni, LRF; Silva, WC; Santos, AA; Alves, FAF; Bezerra, IRS; Potencial de gramíneas forrageiras na fitorremediação de chumbo por meio da produção de fitólitos em solos contaminados. *Land* 2023, 12, 62. <https://doi.org/10.3390/land12010062>

FERNANDES, A. R.; SANTOS, E. S.; DE SOUZA BRAZ, A. M.; BIRANI, S. M.; ALLEONI, L. R. F. Quality reference values and background concentrations of potentially toxic elements in soils from the Eastern Amazon, Brazil. *Journal of geochemical exploration*, v. 190, p. 453-463, 2018. <https://doi.org/10.1016/j.gexplo.2018.04.012>

García, C., Fernández, J., Asto, A.; García G., H. Organic matter in soils: Implications for metal mobility and availability. *Environmental Science & Technology*, 55(3), 1234-1241. 2019. DOI: 10.1021/acs.est.0c06250.

Gee, G.W., Bauder, J.W., 1986. Methods of Soil Analysis.

Godwyn-Paulson, P., Jonathan, M.P., Rodríguez-Espinosa, P.F., Rodríguez-Figueroa, G.M., 2022. Rare earth element enrichments in beach sediments from Santa Rosalia mining region, Mexico: An index-based environmental approach. *Mar. Pollut. Bull.* 174, 113271. <https://doi.org/10.1016/j.marpolbul.2021.113271>

Hakanson, L., 1980. An ecological risk index for aquatic pollution control.a sedimentological approach. *Water Res.* [https://doi.org/10.1016/0043-1354\(80\)90143-8](https://doi.org/10.1016/0043-1354(80)90143-8)

Huang, X., Li, Y., & Wang, Y. (2020). Effects of soil texture on heavy metal retention and availability in mining areas. *Soil and Tillage Research*, 204, 104756. DOI: 10.1016/j.still.2020.104756.

INSTITUTO BRASILEIRO DE GEOGRAFIA E ESTATÍSTICA. *Rebanhos e valor dos principais produtos de origem animal foram recordes em 2022*. Rio de Janeiro: IBGE, 2023. Disponível em: <https://agenciadenoticias.ibge.gov.br>. Acesso em: 01 nov. 2024.

Jean-Lavénir, N.M., Kiki, T.N., Yiika, L.P., Ndi, G.M., 2023. Contamination, sources and risk assessments of metals in stream sediments of Pouma area, Pan-African Fold Belt, Southern Cameroon. Water. Air. Soil Pollut. 234, 160. <https://doi.org/10.1007/s11270-023-06180-4>

Jiménez-Ballesta, R., Bravo, S., Amorós, J.Á., Pérez-De-Los-Reyes, C., García-Pradas, J., Sanchez, M., García-Navarro, F.J., 2022. Occurrence of some rare earth elements in vineyard soils under semiarid Mediterranean environment. Environ. Monit. Assess. 194, 341. <https://doi.org/10.1007/s10661-022-09956-z>

Khan, R., Islam, Md.S., Tareq, A.R.M., Naher, K., Islam, A.R.Md.T., Habib, Md.A., Siddique, Md.A.B., Islam, M.A., Das, S., Rashid, Md.B., Ullah, A.K.M.A., Miah, Md.M.H., Masrura, S.U., Bodrud-Doza, Md., Sarker, M.R., Badruzzaman, A.B.M., 2020. Distribution, sources and ecological risk of trace elements and polycyclic aromatic hydrocarbons in sediments from a polluted urban river in central Bangladesh. Environ. Nanotechnol. Monit. Manag. 14, 100318. <https://doi.org/10.1016/j.enmm.2020.100318>

Kumar, V., Sharma, A., Pandita, S., Bhardwaj, R., Thukral, A.K., Cerda, A., 2020. A review of ecological risk assessment and associated health risks with heavy metals in sediment from India. Int. J. Sediment Res. 35, 516–526. <https://doi.org/10.1016/j.ijsrc.2020.03.012>

Liu, J., Dai, S., Berti, D., Eble, C.F., Dong, M., Gao, Y., Hower, J.C., 2023. Rare Earth and Critical Element Chemistry of the Volcanic Ash-fall Parting in the Fire Clay

Coal, Eastern Kentucky, USA. *Clays Clay Miner.* 71, 309–339.

<https://doi.org/10.1007/s42860-023-00237-5>

López-Piñeiro, A., Cárdenas, M., & García-Montoya, E. The role of organic matter in the mobility of heavy metals in contaminated soils: A review. *Soil Biology and Biochemistry*, 154, 108147. (2021). DOI: 10.1016/j.soilbio.2020.108147.

Lu, X., Zhang, X., Li, L.Y., Chen, H., 2014. Assessment of metals pollution and health risk in dust from nursery schools in Xi'an, China. *Environ. Res.* 128, 27–34.

<https://doi.org/10.1016/j.envres.2013.11.007>

Lima, M.W. De, Pereira, W.V. Da S., Souza, E.S. De, Teixeira, R.A., Palheta, D. Da C., Faial, K. Do C.F., Costa, H.F., Fernandes, A.R., 2022. Bioaccumulation and human health risks of potentially toxic elements in fish species from the southeastern Carajás Mineral Province, Brazil. *Environ. Res.* 204, 112024.

<https://doi.org/10.1016/j.envres.2021.112024>

Matlaba, V. J.; Maneschy, M. C.; Santos, J. F.; Mota, J. A. Socioeconomic dynamics of a mining town in Amazon: a case study from Canaã dos Carajás, Brazil. *Mineral Economics.* 32, 75– 90, 2019.

<https://doi.org/10.1007/s13563-018-0159-6>

Moreira, L.J.D., da Silva, E.B., Fontes, M.P.F., Liu, X., Ma, L.Q., 2018. Speciation, bioaccessibility and potential risk of chromium in Amazon forest soils. *Environ. Pollut.* 239, 384–391. <https://doi.org/10.1016/j.envpol.2018.04.025>

Neto, H. F. S.; Pereira, W. V. S.; Dias, Y. N.; Souza, E. S.; Teixeira, R. A.; Lima, M. W.; Ramos, S. J.; Amarante, C. B.; Fernandes, A. R. Environmental and human health risks of arsenic in gold mining areas in the eastern Amazon. *Environmental pollution*, v. 266, p. 114969, 2020.

Pereira, W.V. Da S., Ramos, S.J., Melo, L.C.A., Dias, Y.N., Martins, G.C., Ferreira, L.C.G., Fernandes, A.R., 2023. Human and environmental exposure to rare earth

elements in gold mining areas in the northeastern Amazon. Chemosphere 340, 139824. <https://doi.org/10.1016/j.chemosphere.2023.139824>

Pereira, W.V. Da S., Ramos, S.J., Melo, L.C.A., Braz, A.M. De S., Dias, Y.N., Almeida, G.V. De, Fernandes, A.R., 2022. Levels and environmental risks of rare earth elements in a gold mining area in the Amazon. Environ. Res. 211, 113090. <https://doi.org/10.1016/j.envres.2022.113090>.

R Core Team, 2023. R: A language and environment for statistical computing.

Sergeeva, A., Zinicovscaia, I., Grozdov, D., Yushin, N., 2021. Assessment of selected rare earth elements, HF, Th, and U in the Donetsk region using moss bags technique. Atmospheric Pollut. Res. 12, 101165. <https://doi.org/10.1016/j.apr.2021.101165>

Souza Neto, H.F. De, Pereira, W.V. Da S., Dias, Y.N., Souza, E.S. De, Teixeira, R.A., Lima, M.W. De, Ramos, S.J., Amarante, C.B. Do, Fernandes, A.R., 2020. Environmental and human health risks of arsenic in gold mining areas in the eastern Amazon. Environ. Pollut. 265, 114969. <https://doi.org/10.1016/j.envpol.2020.114969>

Silva, Fernanda Rodrigues Da., Barros, M. A. S. A., Pierosan, R., Pinho, F. E. C., Rocha, M. L. B. P., Vasconcelos, B. R., Dezula, S. E. M., Tavares, C., Rocha, J. Geoquímica e geocronologia UCPb (SHRIMP) de granitos da região de Peixoto de Azebedo: Proíncia Aurífera Alta Floresta, Mato Grosso. Brazilian Journal of Geology, São Paulo, i. 44, n. 3, p. 433C455, jul./set. 2014. <http://dx.doi.org/10.5327/22317C4889201400030007>.

Saha, B., Eliason, K., Golui, D., Masud, J., Bezbaruah, A.N., Iskander, S.M., 2023. Rare earth elements in sands collected from Southern California sea beaches. Chemosphere 344, 140254. <https://doi.org/10.1016/j.chemosphere.2023.140254>

Saleh, H.M., Eskander, S.B., Mahmoud, H.H., Abdelaal, S.A., 2022. Study on rare earth elements, heavy metals and organic contents in the soil of oil exploration site at Matruh Governorate, Egypt. Results Geophys. Sci. 9, 100039.

<https://doi.org/10.1016/j.ringps.2021.100039>

Sutherland, R.A., 2000. Bed sediment-associated trace metals in an urban stream, Oahu, Hawaii. Environ. Geol. 39, 611–627.

Sojka, M., Choiński, A., Ptak, M., Siepak, M., 2021. Causes of variations of trace and rare earth elements concentration in lakes bottom sediments in the Bory Tucholskie National Park, Poland. Sci. Rep. 11, 244. <https://doi.org/10.1038/s41598-020-80137-z>

Sun, G., Li, Z., Liu, T., Chen, J., Wu, T., Feng, X., 2017. Rare earth elements in street dust and associated health risk in a municipal industrial base of central China. Environ. Geochem. Health 39, 1469–1486. <https://doi.org/10.1007/s10653-017-9982-x>

Wang, Y., Wang, G., Sun, M., Liang, X., He, H., Zhu, J., Takahashi, Y., 2022. Environmental risk assessment of the potential “Chemical Time Bomb” of ion-adsorption type rare earth elements in urban areas. Sci. Total Environ. 822, 153305. <https://doi.org/10.1016/j.scitotenv.2022.153305>

Teixeira, P.C., Donagemma, G.K., Fontana, A., Teixeira, W.G., 2017. Manual de métodos de análise de solo, 3. ed. rev. ed. Embrapa, Brasília, DF.

Tomlinson, D.L., Wilson, J.G., Harris, C.R., Jeffrey, D.W., 1980. Problems in the assessment of heavy-metal levels in estuaries and the formation of a pollution index. Helgoländer Meeresunters. 33, 566–575. <https://doi.org/10.1007/BF02414780>

USEPA, 2001. Supplemental guidance for developing soil screening levels for superfund sites. Office of Solid Waste and Emergency Response, Washington

Veiga, M. M., Salazar, H. M. S. C., de Lima, D. J. C. (2014). Artisanal and small-scale gold mining and the environment: A review. *Science of the Total Environment*, 466, 785–797. <https://doi.org/10.1016/j.scitotenv.2013.12.049>

Zerizghi, T., Guo, Q., Wei, R., Wang, Z., Du, C., Deng, Y., 2023. Rare earth elements in soil around coal mining and utilization: Contamination, characteristics, and effect of soil physicochemical properties. *Environ. Pollut.* 331, 121788.  
<https://doi.org/10.1016/j.envpol.2023.121788>

## **Material suplementar**

**Tabela 1.**

Características químicas e granulométricas de resíduos de minas artesanais de exploração de cassiterita e monazita.

Áreas	Propriedades					
	pH (H <sub>2</sub> O)	MO (g dm <sup>-3</sup> )	CTC (cmol <sub>c</sub> dm <sup>-3</sup> )	Argila g	Areia	Silte
TA1	4.5 ± 0.2	20.0 ± 8.3	1.4 ± 0.3	16.7 ± 8.6	74.9 ± 14.3	8.4 ± 6.4
TA2	4.6 ± 0.2	25.0 ± 0.4	1.1 ± 0.1	23.4 ± 2.6	54.1 ± 7.7	22.5 ± 5.7
TA3	4.8 ± 0.1	25.7 ± 2.9	1.2 ± 0.3	33.8 ± 3.3	58.1 ± 4.9	8.1 ± 4.6
RA	4.9 ± 0.1	57.7 ± 3.4	2.3 ± 0.1	44.4 ± 0.4	41 ± 0.5	14.5 ± 0.2

MO = matéria organica; CTC = capacidade de troca de cátions.

**Tabela 2S.**

Locais de amostragem

Areas	Sample	Latitude (S)	Longitude (W)
TA1	S1	06°04'12"S	52°11'24"W
	S2	06°04'15.6"S	52°11'27.6"W
	S3	06°04'22.8"S	52°11'27.6"W
	S4	06°04'30"S	52°11'31.2"W
	S5	06°04'44.4"S	52°11'31.2"W
	S6	06°04'37.2"S	52°11'34.8"W
	S7	06°04'9.6"S	52°11'38.4"W
	S8	06°04'2404"S	52°11'49.2"W
TA2	S1	06°02'2.4"S	52°14'27.6"S
	S2	06°02'20.4"S	52°14'31.2"S
	S3	06°02'27.6"S	52°14'27.6"S
TA3	S1	06° 03'18"S	52°10'51.6"S
	S2	06° 03'36"S	52°10'50.2"S
	S3	06° 03'33"S	52°10'48"S
RA	S1	06°04'30"S	52°09'57.6"S
	S2	06°04'15.6"S	52°09'37.4"S
	S3	06°04'44.4"S	52°09'37.6"S